Spring 5-2-2023

Does VDAC2 Have A BH3 Domain?

Lillian Ferkany
University of Mississippi

Does VDAC2 Have A BH3 Domain?

By
Lillian Ferkany

A Thesis Submitted to The University in Mississippi in partial fulfillment of the requirements of the Sally McDonnell Barksdale Honors College.

Oxford
May 2023

Approved By:

_____
Advisor: Dr. Mika Jekabsons

_____
Reader: Dr. Bradley Jones

_____
Reader: Dr. Joshua Bloomekatz

ACKNOWLEDGEMNTS

I would like to thank Dr. Mika Jekabsons for his mentorship and support. I am grateful to have had the opportunity to perform research under his guidance, and to have learned so much while assisting in his lab. Additionally, I would like to thank him for his instruction, patience, and encouragement while working on this project, as well as for supporting my future endeavors. I would also like to thank Claire Pearsons for her support on this project.

ABSTRACT

Lillian Ferkany: Does VDAC2 Have a BH3 Domain?
(Under the direction of Dr. Mika Jekabsons)

Mitochondrial outer membrane permeabilization (MOMP) by Bax oligomerization triggers apoptosis. BCl-2 family proteins, classified as BH3 only proteins, pro-survival proteins, or pro-apoptotic proteins, control apoptosis partly through their agonist or antagonistic effects on Bax, which are mediated by their conserved BH3 domains. All BH3 domains form an alpha helix containing 5-7 conserved hydrophobic residues, designated H0-H5, and one conserved aspartic acid that drive interaction with Bax and other 'multi-domain' BCl-2 members. BH3 agonists induce Bax oligomerization, while BH3 antagonists sequester Bax to prevent MOMP. We discovered that voltage dependent anion channels (VDACs) in the MOM contain a putative BH3-like domain based on sequence similarity with known BH3 domains. This study tested the hypothesis that the VDAC2 isoform contains a functional BH3 domain that binds recombinant Bax in a manner similar to the Bim BH3 domain. Using fluorescent-tagged synthetic peptides, Bax bound VDAC2, but with a 4-fold lower affinity than the Bim BH3 domain. The conserved aspartate was important for this interaction, as substitution with arginine at this position reduced Bax affinity by 2.6-fold. A proline at the H0 position also promoted Bax binding to VDAC2. All known BH3 domains have a conserved leucine at the H2 position, but this is shifted one residue closer to H1 in VDAC2. Substitution of leucine for a smaller hydrophobic alanine at H2 substantially lowered the K_D, suggesting the non-conserved position of the H2 Leu contributed to Bax's lower affinity for VDAC2, along with the large aromatic residues at H1 (Tyr), H4

(Phe), and H5 (Phe). The N-terminus of VDAC2 thus has the essential elements of a BH3 domain, but the combination of residues at the conserved positions make it less well suited for binding to Bax.

TABLE OF CONTENTS

LIST OF FIGURES

INTRODUCTION

Apoptosis has a crucial physiological function by genetically eliminating excess cells during development, and dead or damaged cells in mature tissues to maintain homeostasis (Elmore, 2007). The genes controlling apoptosis distinguishes this process from other forms of cell death such as necroptosis, which is the alternative cellular death pathway. The origin of the cellular stress signal, tissue type, and developmental stage are all key factors in determining if a cell will proceed with either apoptotic or another form of regulated cell death (Elmore, 2007). Apoptosis can proceed through either an extrinsic mechanism where signaling pathways involve transmembrane receptors that are members of the tumor necrosis factor (TNF) family, or it can proceed through an intrinsic pathway which involves the BCl-2 family and permeabilization of the mitochondria (Elmore, 2007). Morphological changes occur at a subcellular level during apoptosis that include nuclear condensation, fragmentation of genomic DNA, and membrane blebbing. The mitochondria are known to play a dual role in determining the fate of a cell by generating ATP via oxidative phosphorylation, thus prolonging the cells survival by providing energy, or through release of apoptosis-inducing factors such as cytochrome c, via the intrinsic pathway, leading to apoptosis and subsequent cellular death (Westphal et al, 2014). This study focuses on the intrinsic apoptotic pathway, and specifically the role of the voltage-dependent anion channel isoforms (VDACs) and their interactions with the BCl-2 family member Bax as a possible regulatory step in either inducing or suppressing apoptosis.

BCl-2 family proteins are important determinates of apoptosis through the balance of their interactions with each other and the mitochondria (Czabotar et al, 2014). The

BCl-2 family has three distinct subsets of proteins; the pro-apoptotic BH3-only proteins, pro-survival proteins, and pro-apoptotic effector proteins. BH3 only proteins contain a BCl-2 homology 3 (BH3) domain through which they activate the pro-apoptotic effectors to initiate apoptosis. The pro-survival proteins, such as BCl-2, BCl-xL, and MCl-1, protect cells from apoptosis by sequestering the pro-apoptotic effectors in an inactive state (Czabotar et al., 2014). The pro-apoptotic effector proteins Bax and Bak undergo conformational changes that cause them to oligomerize within the mitochondrial outer membrane (MOM) upon interaction with activator BH3 only family members, thus activating the process of cytochrome c release from mitochondria (Czabotar et al., 2014). Both Bax and Bak, contain a BH3 domain that is involved in their conversion from harmless monomers to harmful oligomers within the MOM. Cytochrome c exits the mitochondria through the oligomeric pores formed by Bax and Bak, which activates caspases that trigger cell death (Hardwick et al. 2013, Westphal et al. 2014). Cytochrome c itself has a twofold function when it is translocated to the cytoplasm; the loss of cytochrome c in the mitochondria disables cellular energy production, and because cytochrome c activates proteolytic caspases, it causes degradation of many proteins necessary for cell function (Westphal et al, 2014). The model of apoptosis regulation via BCl-2 family members includes anti-apoptotic protein sequestration of the BH3 α-helical domain of a pro-apoptotic effector through binding to a surface hydrophobic groove of the anti-apoptotic member (Hardwick et al, 2013). The sequestration of the Bax or Bak BH3 domain by a pro-survival protein prevents Bax or Bak BH3 domain-mediated oligomeric assembly within the MOM.

Beyond their association with apoptotic pathways, BCl-2 family members are thought to have noncanonical functions including their ability to change the shape and energetics of mitochondria, the regulation of autophagy, and the ability to initiate immunity when cells are exposed to viruses (Hardwick et al, 2013). This study is focused on understanding the physiological significance of BCl-2 family member interactions, as mutations in one or more of these genes are known to be associated with cancer, developmental defects, and neurodegeneration. Understanding how they are activated, inhibited, and regulated not only provides insight into basic cell biology, but also opportunities to develop customized and selective drugs that can activate or suppress apoptotic processes in targeted cells to mitigate pathological conditions (Westphal et al, 2014). Most multi-BH domain family members fold to form a surface hydrophobic groove, which functions as a receptor site that binds to the BH3 domain of other BCl-2 family members. The exact structure of the hydrophobic groove varies with each member, and this is turn affects how strongly a particular multi-BH domain protein may bind to another family member. This groove has become a primary target for the development of therapies that selectively bind to one or more of the family members to either inhibit or stimulate activity. The hydrophobic groove of Bax is of particular interest since binding of some BH3 domains (e.g., Bim, Bid) to this site triggers conformational changes that drive oligomerization and apoptosis. The structural requirements for BH3 domains or other ligands that lead to Bax activation or inhibition are important to understanding Bax regulation and the possible development of treatment for diseases such as cancer. The focus of this research is to identify if VDAC2 contains a BH3 domain allowing it to bind to pro-apoptotic BCl-2 family members and proposing a new

approach to pharmaceutical control of apoptosis via BCL-2 family interactions at the mitochondrial membrane.

VDAC2 is a 19-beta strand mitochondrial outer membrane protein important for metabolism (Bayrhuber et al. 2008). It forms small, relatively non-specific beta-barrel pore in the MOM that allows diffusion of metabolites such as pyruvate, malate, and ADP between the cytoplasm and the mitochondrial intermembrane space. A number of studies have implicated VDACs in apoptosis regulation, as both Bak and Bax have been found to form complexes with VDAC2 and/or VDAC1 (Cheng et al 2003, Huckabee and Jekabsons 2011, Ma et al 2014) (Yuan et al., 2021). Yuan and colleagues have suggested that VDACs are not required for apoptosis but may instead be important tethering sites for Bax or Bak at the MOM. VDAC2 is not required, but still helpful, for Bak-mediated apoptosis, however, there is some evidence suggesting it may be required for Bax-mediated apoptosis (Yuan, 2021). Yuan and his colleagues concluded that VDAC2 is not a BCl-2 family member, but that it is involved in the process of Bax and Bak regulation, which in turn mediate apoptosis (Yuan et al. 2021). However, the exact structural determinants of VDAC2 interaction with Bax and Bak remain unclear. We recently discovered strong sequence similarities of the N-terminus of VDAC2 with BH3 domains, raising the possibility that VDAC2 interacts with Bax through this conserved sequence. The goal of this study is to determine if VDAC2 contains a functional BH3 domain and is thus a novel member of the BCl-2 family. For this, recombinant Bax binding to a series of VDAC2 peptides was determined to evaluate the relative importance of specific residues that constitute the putative BH3 domain with those shown to be important in known BH3 domains.

METHODS

A. Recombinant Bax

Recombinant human Bax (hereafter referred to as Bax) with the final twenty-one amino acids deleted (truncated at Gln171) was purchased from Creative Biomart (Shirley, New York; catalog number Bax6976H) in liquid form containing 5 % trehalose, 30 % glycerol, 150 mM NaCl, 20 mM phosphate buffer pH 7.2, and 2 mM EDTA). Truncation at Gln171, which deletes the ninth α-helix, improves solubility and exposes the canonical hydrophobic groove for binding analysis. The recombinant protein contains 6-histidine tags on both the N- and C-termini to facilitate purification.

B. Synthetic Peptides

All wild type and mutant custom 26-mer peptides (90 % purity) were purchased from Mimotopes Inc. (Victoria, Australia). They were fluorescently labeled at the N terminus with 5-carboxyflouresceine with an aminohexinoic acid linker separating the tag from the peptide. Bim peptide stocks (1-2 mM) were dissolved in 80 mM NH_4HCO_3 with 20 % acetonitrile and further diluted in 80 mM NH_4HCO_3, 20 % methanol (5-320 μM stocks). VDAC2 peptide stocks (1-2 mM) were dissolved in 0.1 % acetic acid, 20 % acetonitrile, and further diluted in 0.1 % acetic acid, 20 % methanol (5-320 μM stocks). All stocks were stored at -80^{o}C.

C. Pretreatment of Bax With Octylglucoside

Bax (32.4 μM, 0.72 mg/mL) or vehicle (150 mM NaCl, 30 % glycerol, 5 % trehalose, 20 mM TES pH 7.3, and 2 mM EDTA) was diluted 1:3 in binding buffer (150 mM KCl, 20

mM TES pH 7.3, 3 mM EDTA, 1 mM DTT, and 0.5 % octylglucoside) and incubated on ice for 2-3 hours prior to binding studies.

D. Equilibrium binding

After preincubation, triplicate 1:3 Bax or vehicle (1.83 μL) were added to 178.2 μL of binding buffer solution supplemented with different peptide concentrations. The samples were incubated for 1 hr at 3º C on an orbital shaker (130 rpm). Bim or VDAC2 peptide standards in binding buffer were run in parallel. Samples were transferred into 10 kDa Vivaspin PES spin filters and centrifuged for 70-90 seconds, 3ºC and 12,000 xg. The length of time for spinning samples was determined based on the concentration of peptide. Lower concentrations were spun for 70-75 seconds, and higher concentrations were spun for 80-90 seconds so that approximately 40-50 % of sample volume was filtered. Filtrate fluorescence was then quantified using a spectrofluorophotometer (Shimadzu RF6000), with λex set to 494 nm and λem set to 524 nm. The amount of peptide bound to Bax was calculated as

Amount Bound (fmol) = ($[peptide]_{veh}$ x 180 μL) – ($[peptide]_{Bax}$ x 180 μL)

Fluorescence of unfiltered standards was also quantified to determine the fraction of peptide filtered by the spin filters.

Fraction Filtered = ($[peptide]_{filtrate}$)/ ($[peptide]_{total}$)

E. Blue Native Gel Electrophoresis

Peptides (120 μM) were incubated in binding buffer for 2-3 hr at 3o C on an orbital shaker. Aliquots (10 μL) of peptide were mixed with 3 μL of blue native loading buffer (100 mM BisTris pH 7.0, 40 % glycerol) and 2 μL 5% Coomassie G250 dye. The samples were loaded onto 3.6 % stacking, 13-20 % resolving native acrylamide gels

containing 50 mM BisTris pH 7.0, 500 mM aminocaproic acid and electrophoresed for 1 hour and 40 minuets at 3ºC from 100-300 volts. The cathode buffer contained 15 mM BisTris, 50 mM Tricine pH 7.0, with 0.02 % Coomassie G250. The anode buffer contained 50 mM BisTris pH 7.0. The gels were de-stained in 40% methanol and 10% acetic acid and photographed using an Azure 600 gel doc.

RESULTS

The BCl-2 homology 3 (BH3) domain is characterized by 5-7 hydrophobic residues (designated H0 to H5) distributed over twenty amino acids and a single conserved Asp residue between H3 and H4 (Bim, Fig. 1). The N-terminus of VDAC2 is notably similar, with only the conserved Leu at position H2 offset one position closer to H1. Given this similarity to Bim and other BCl-2 family members, a series of 26-mer VDAC2 peptides were tested for their ability to bind to recombinant Bax (Fig. 1).

				H0				H1				H2			H3				H4			H5					
Bim	D	L	R	P	E	I	R	I	A	Q	E	L	R	R	I	G	D	E	F	N	E	T	Y	R	R	-	-	-
BIM H2m	D	L	R	P	E	I	R	I	A	Q	E	A	R	R	I	G	D	E	F	N	E	T	Y	R	R	-	-	-
BIM4xEm	D	L	R	P	E	I	R	E	A	Q	E	E	R	R	E	G	D	E	E	N	E	T	Y	R	R	-	-	-
VDAC2	-	-	-	I	P	P	P	Y	A	D	L	G	K	A	A	R	D	I	F	N	K	G	F	G	F	G	L	V
VDAC2S	-	-	S	I	P	P	P	Y	A	D	L	G	K	A	A	R	D	I	F	N	K	G	F	G	F	G	L	V
VDAC2S H0H2m	-	-	S	I	P	G	P	Y	A	D	A	G	K	A	A	R	D	I	F	N	K	G	F	G	F	G	L	V
VDAC2S H1H3m	-	-	S	I	P	P	P	A	A	D	L	G	K	A	G	R	D	I	F	N	K	G	F	G	F	G	L	V
VDAC2S H2H4m	-	-	S	I	P	P	P	Y	A	D	A	G	K	A	A	R	D	I	G	N	K	G	F	G	F	G	L	V
VDAC2S H3H5m	-	-	S	I	P	P	P	Y	A	D	L	G	K	A	G	R	D	I	F	N	K	G	A	G	F	G	L	V
VDAC2S Dm	-	-	S	I	P	P	P	Y	A	D	L	G	K	A	A	R	R	I	F	N	K	G	F	G	F	G	L	V
VDAC2S4xEm	-	-	S	I	P	P	P	E	A	D	E	G	K	A	E	R	D	I	E	N	K	G	F	G	F	G	L	V

Figure 1A. Sequences of all peptides tested in this study. Conserved hydrophobic residues within the BH3 domain of Bim are labeled H0-H5 and highlighted in blue. Residue H2 is a strictly conserved Leu for all Bcl-2 family members, as is an Asp residue (in red) between H3 and H4. From alignment of the VDAC2 N-terminus with Bim and other BH3 domains (not shown), a similar set of hydrophobic residues (highlighted blue) and a conserved Asp (in red) were identified. Specific amino acid substitutions (orange highlighted boxes), were introduced to test their importance in peptide binding to recombinant Bax .

Table 1 summarizes results from all titration experiments for each peptide tested. Dissociation constants (K_D), which reflect binding affinities, and Hill numbers, which reflect binding cooperativity between receptor sites, were determined by non-linear regression assuming either one or two receptor sites per monomer. Maximum amount

bound (B_{max}), the point at which all receptor sites are bound with peptide, was calculated from the concentration of recombinant Bax used, assuming either one or two receptor sites per monomer.

	K_D (nM)		B_{max} (fmol)		Hill Number	
	1 Site	2 Sites	1 Site	2 Sites	1 Site	2 Sites
VDAC2	-	-	-	-	-	-
VDAC2 WT	984	2,550	19,800	39,600	1.99	1.31
VDAC2S	1,048	1,938	19,800	39,600	2.06	2.10
VDAC2S [H_0H_2] Mutant	1,061	3,824	19,800	39,600	1.19	0.93
VDAC2S [H_1H_3] Mutant	602	1,552	19,800	39,600	1.82	1.38
VDAC2S [H_2H_4] Mutant	128	287	19,800	39,600	2.41	1.66
VDAC2S [H_3H_5] Mutant	739	2,353	19,800	39,600	1.44	1.08
VDAC2S [D] Mutant	2,649	7,641	19,800	39,600	1.09	0.96
VDAC2S [4xE] Mutant	761	2,073	19,800	39,600	1.58	1.24
Bim	-	-	-	-	-	-
Bim WT	216	484	19,800	39,600	1.96	1.60
Bim [H_2] Mutant	928	1,408	19,800	39,600	6.00	2.42
Bim [4xE] Mutant	875	1,721	19,800	39,600	2.0	2.0

Table 1. Calculated dissociation constants (K_d) in nM, maximum bound (B_{max}) in fmol, and hill coefficents for all WT and mutant Bim and VDAC2 peptides.

A. Bim Peptides

Bim is an important pro-apoptotic protein that activates BAX through binding of its BH3 domain to a hydrophobic groove formed by Bax α-helices 2-5. The Bim BH3 domain peptide was thus used as a positive control from which to compare Bax binding to VDAC2

peptides. Bax affinity for wild type Bim peptide (Fig 2A) ranged from 216-484 nM, depending on whether a 1- or 2-site model was used to determine K_d by non-linear regression (Table 1). The correlation coefficients from the analysis indicate the 2-site model is a better fit to the data ($R^2 = 0.469$; one site, and $R^2 = 0.662$; two sites, Fig 2A). Non-linear regression analysis constrained to a maximum binding of 19,800 or 39,600 fmol (B_{max} for 1 or 2 sites, respectively, based on 110 nM Bax added) were used for the analysis based on a few reports indicating that Bax has two distinct BH3 domain receptor sites (Gavothiotis et al 2008, Hauseman et al 2020). It is worth highlighting that the average amount of bound peptide exceeded that expected for two sites per monomer at the highest concentrations of peptide (Fig 2A), suggesting that either non-specific binding to protein contaminants has occurred, or the stock Bax concentration is higher than reported by the manufacturer. For both 1- and 2-site models, the Hill coefficients (n_H) exceeded 1.5, suggesting positive binding cooperativity between Bax monomers for the one site model ($n_H = 1.96$) or between the two sites within each monomer for the two site model ($n_H = 1.60$) (Table 1).

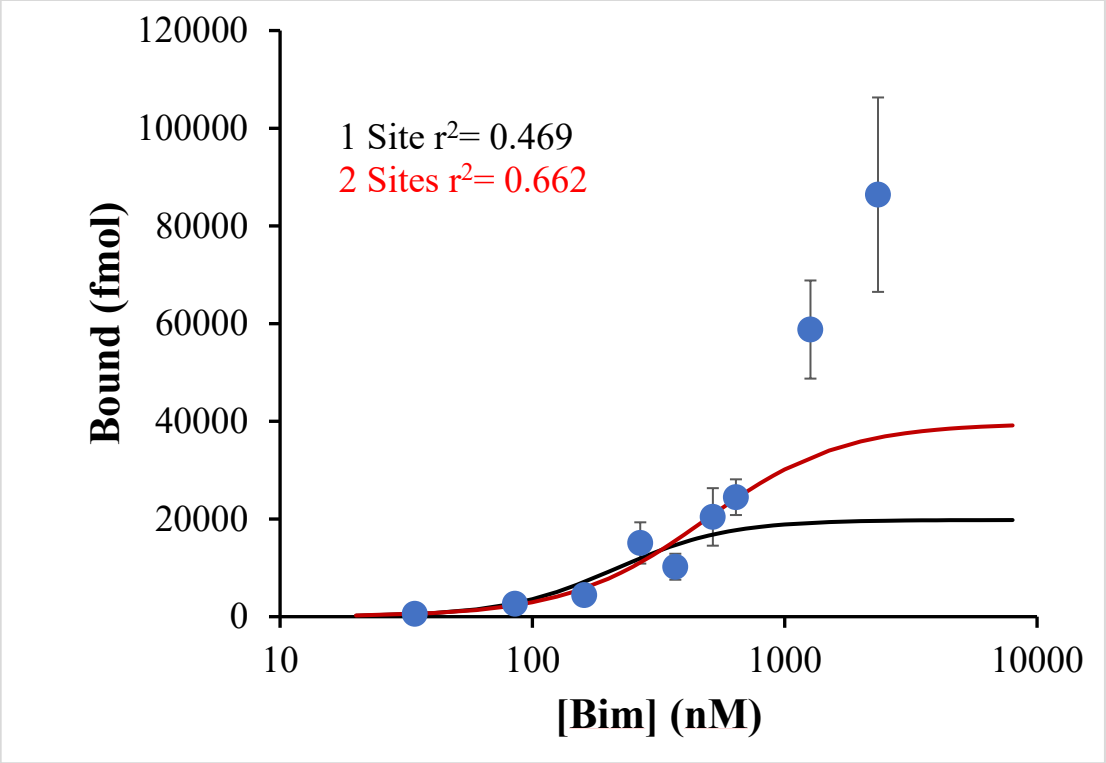

Figure 2. Recombinant Bax binding to wild type Bim peptide. Data are mean ± SEM of 5-8 experiments Non-linear regression curves were fit to the data assuming one binding site per monomer (black, 19800 fmol B_{max}) or two sites per monomer (red, 39600 fmol B_{max}). The correlation coefficient for each regression model is color-coded to the corresponding curve.

Next, we titrated Bax with a Leu→ Ala H_2 mutant Bim peptide which has previously been shown to have a significantly lower affinity for Bax (Czabotar et al., 2014). Both leucine and alanine are hydrophobic, but alanine has a smaller hydrophobic methyl side chain than leucine. Consistent with previous studies (Czabotar et al., 2014), the Bim H_2 mutant had a 2.9-4.3 lower binding affinity than WT Bim, depending on whether the 1- or 2-site models were compared (Table 1, Fig 3B). The 1- and 2-site models fit the data with similar correlation coefficients, although the modestly higher R^2 of the two-site model is consistent with the WT peptide. Maximum measured binding exceeded that expected for one receptor site per monomer but did not exceed that expected for two sites (Fig 3A). Similar to WT

Bim, the hill coefficients indicated positive cooperativity (n_H = 6.0 and 2.4 for 1- and 2-sites, respectively).

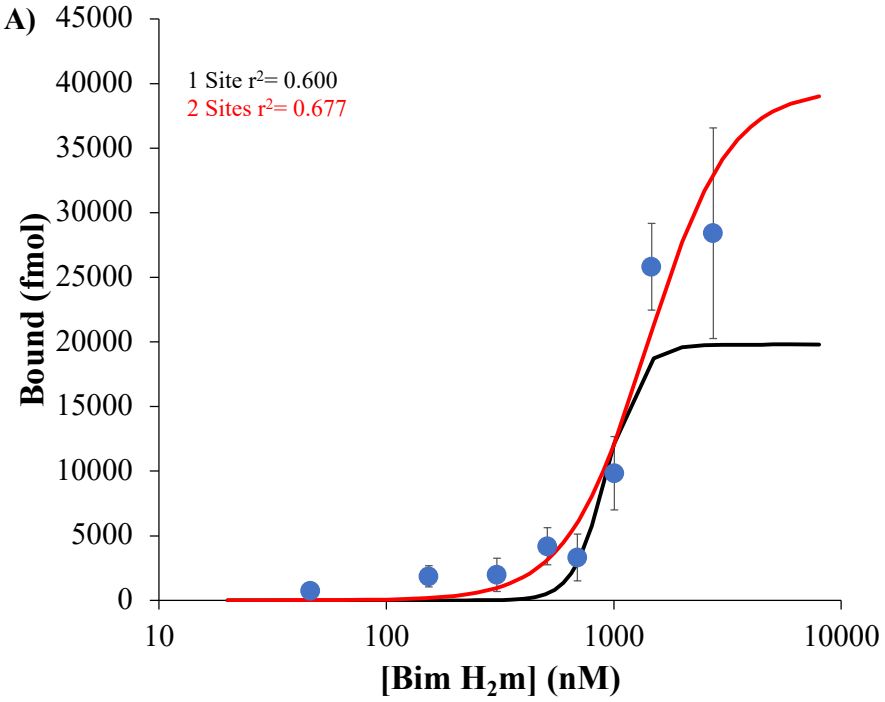

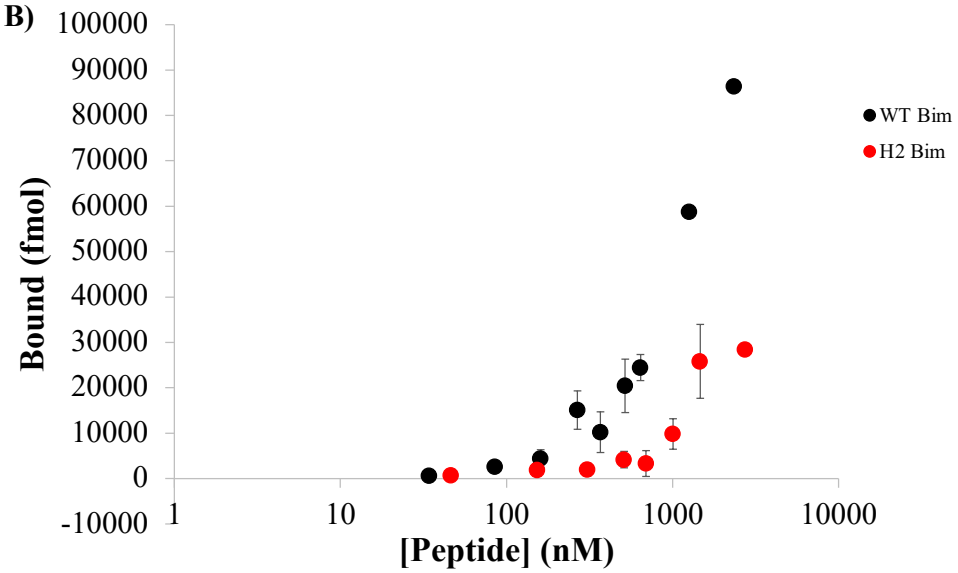

Figure 3. Recombinant Bax binding to Bim H2 mutant peptide. (A) Titration of Bax with Leu→Ala H2 mutant. Non-linear regression curves were fit to the data assuming one binding site per monomer (black, 19800 fmol B_{max}) or two sites per monomer (red, 39600 fmol B_{max}). The correlation coefficient for each regression model is color-coded to the corresponding curve. (B) Overlay of binding curves for wild type and H2 mutant peptides.

Next, we tested a quadruple Bim mutant peptide with four glutamic acid residues substituted for the hydrophobic residues at positions H_1 to H_4 (Fig 1). Surprisingly, Bax affinity for the quadruple mutant was similar to the H2 mutant, with a K_d 4 to 5-fold lower than wild type Bim (Table 1; Fig 4B). The two-site model was again a better fit to the data (Fig 4A; R^2 = 0.415; one site, and R^2 = 0.642; two sites). The Hill coefficients again indicated positive binding cooperativity (Table 1).

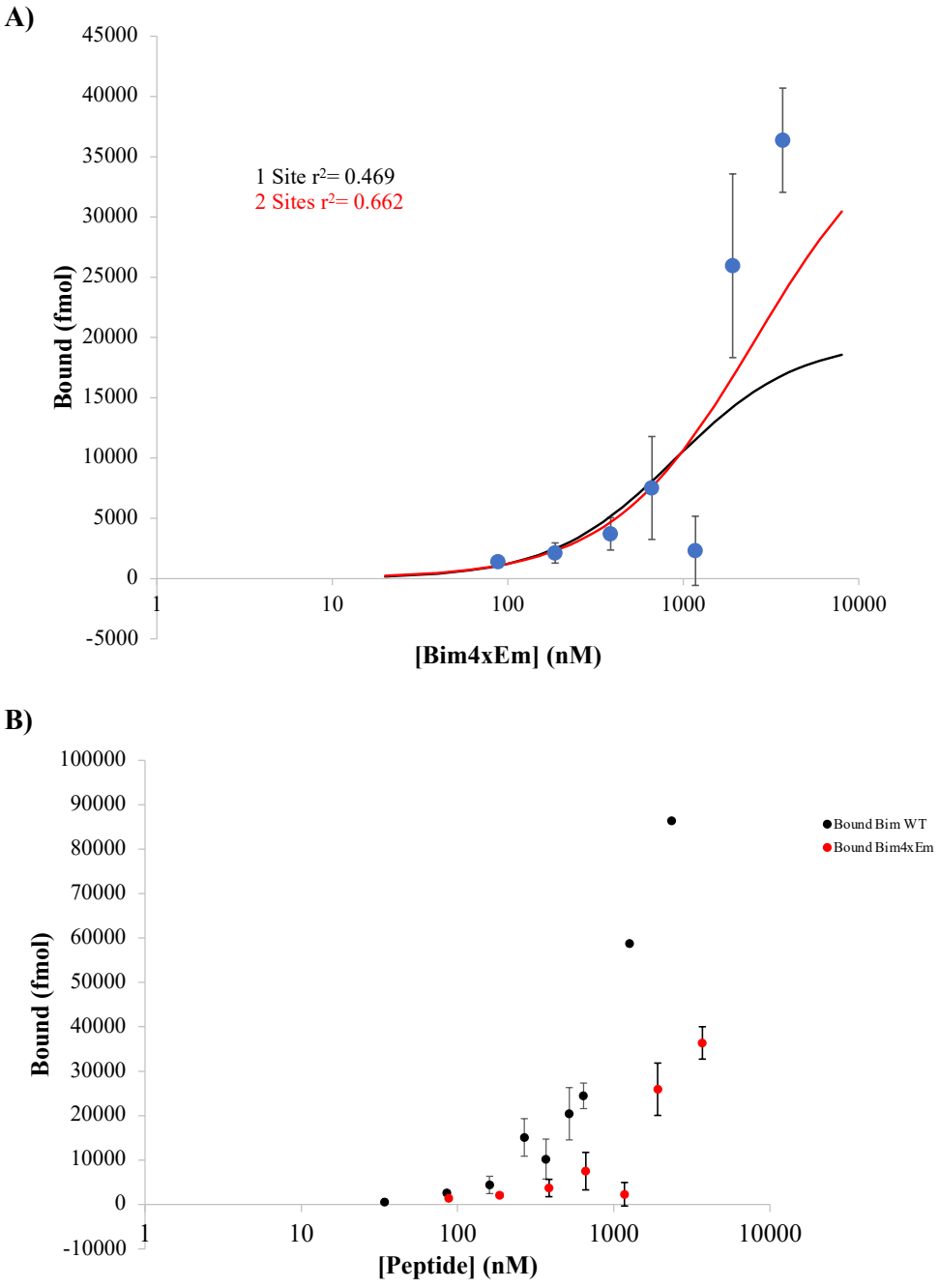

Figure 4. Bax binding to a Bim quadruple mutant peptide. Hydrophobic residues H1, H2, H3, and H4 were mutated to glutamates, with the peptide designated the Bim4xE mutant. (A)Data are mean ± SEM of 5-8 experiments, with each concentration run in triplicate, represented by error bars of bound data values. Non-linear regression curves were fit to the data assuming one binding site per monomer (black, 19800 fmol B_{max}) or two sites per monomer (red, 39600 fmol B_{max}). The correlation coefficient for each regression model is color-coded to the corresponding curve. (B) Overlay of binding curves for wild type and 4xE quadruple mutant peptides. mol).

B. Bax binding to VDAC2 peptides

VDAC2 is a voltage dependent anion channel situated in the mitochondrial outer membrane (MOM) and thus could potentially interact with mitochondrially-associated Bax. The purpose of titrating the VDAC2 WT was to determine if Bax binds to VDAC's putative BH-3 like domain, and if so, which combination of hydrophobic and charged residues are important for binding. For this, we first compared binding of C→S mutant to the wild type peptide (VDAC2S vs. VDAC2 WT, Fig 1). We wanted to determine if the VDAC2S peptide could effectively substitute as the wild type peptide since the Cys residue is prone to oxidation and disulfide bond formation, which could lead to artifacts in binding measurements.

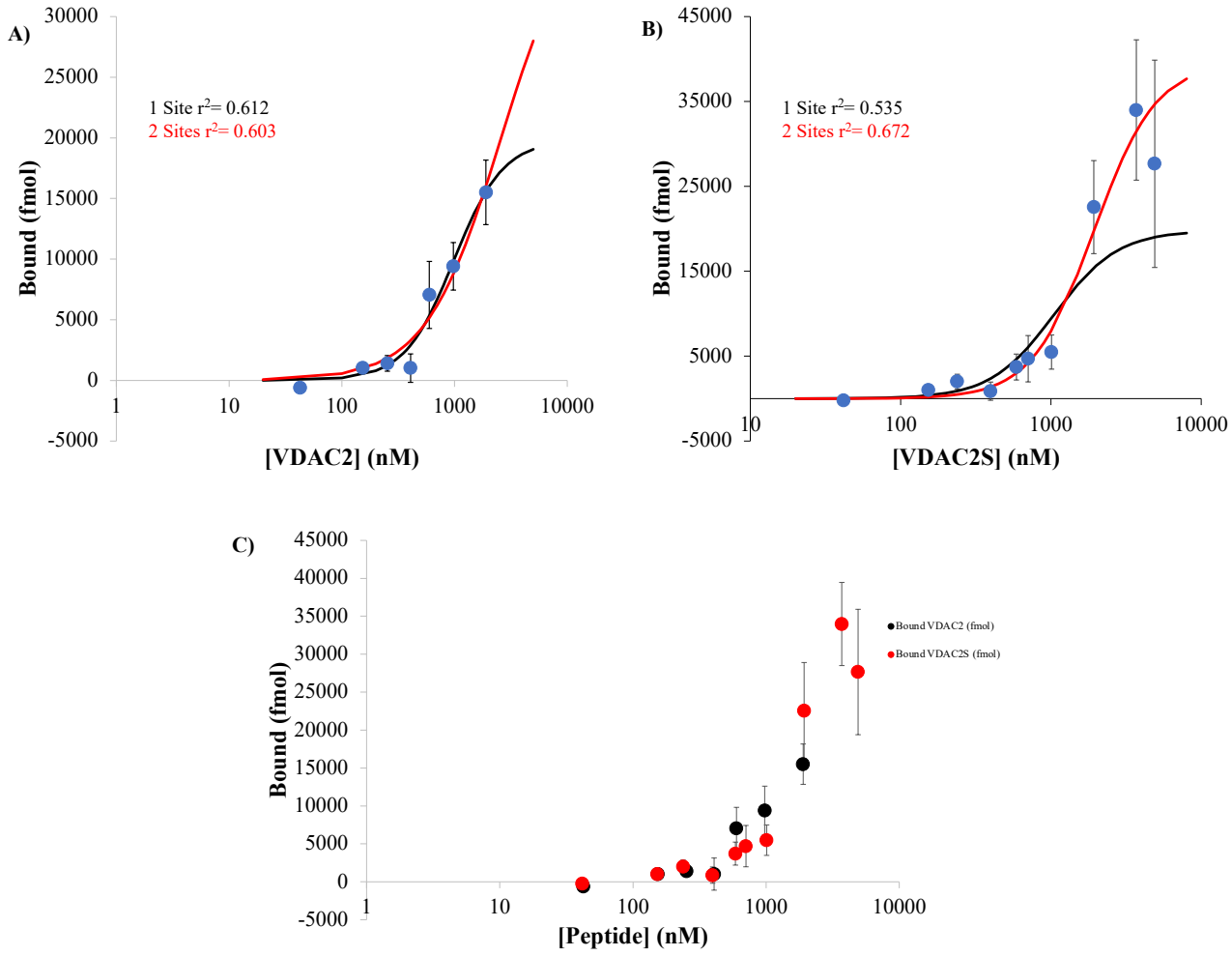

Figure 5. Bax binding to VDAC2 and VDAC2S peptides. C → S mutation at the H0 residue designated the VDAC2S mutant. (A)Data are mean ± SEM of 5-8 experiments of VDAC2, with each concentration run in triplicate, represented by error bars of bound data values. Non-linear regression curves were fit to the data assuming one binding site per monomer (black, 19800 fmol B_{max}) or two sites per monomer (red, 39600 fmol B_{max}). The correlation coefficient for each regression model is color-coded to the corresponding curve. (B) Data are mean ± SEM of 5-8 experiments of VDAC2S, with each concentration run in triplicate, represented by error bars of bound data values. Non-linear regression curves were fit to the data assuming one binding site per monomer (black, 19800 fmol B_{max}) or two sites per monomer (red, 39600 fmol B_{max}). The correlation coefficient for each regression model is color-coded to the corresponding curve. (C) Overlay of binding curves for wild type and VDAC2S mutant peptides.

Titration of Bax with wild type VDAC2 and VDAC2S generally yielded similar affinities and Hill coefficients for both 1- and 2-site fits (Fig 5, Table 1; VDAC2S Kd = 106 and 76 % of WT for 1- and 2-site fits, respectively), although the Hill coefficient for wild type 2-site model indicated no cooperativity while that for VDAC2S and 1-site model for wild type

peptide suggested positive cooperativity. Titration of Bax with wild type peptide over a smaller concentration range than for VDAC2S peptide (43 → 1900 nM vs. 42 → 4900 nM, respectively) resulted in less bound peptide (Fig 5C), which could potentially lead to inaccurate curve fitting; additionally this could explain why the wild type correlation coefficients were essentially the same for the 1- and 2-site models (R2 = 0.612 and 0.603, respectively), whereas the 2-site model was a better fit for VDAC2S (R2 = 0.534 vs. 0.672 for 1- and 2-site models, respectively). From the results, we believe that VDAC2S can be used as a wild type surrogate in these binding experiments for comparison with Bim. Bax bound VDAC2S with 4 to 5-fold lower affinity compared to Bim (Table 1, 2-site Kd = 1938 vs 484 nM for VDAC2S and WT, respectively), while both exhibited positive cooperativity. We then tested a series of VDAC2S double mutants (H_xH_y m, where x and y refer to hydrophobic positions 0 to 5; Fig 1) to assess the contribution of these hydrophobic residues for binding to Bax. The first mutant tested was an H_0H_2 peptide in which Pro → Gly (at H_0+1) and Leu → Ala substitutions were made (Fig 1). The 1- and 2-site models fit equally well to the data (R2 = 0.343 and 0.321, respectively, Fig 6A), but the effect on Bax affinity for this double mutant differed. The 1-site model indicated no change in affinity (Kd = 1061 nM vs 1048 nM for VDAC2S), whereas the 2-site model indicated a 2.0-fold lower affinity (K_d = 3824 nM vs. 1938 nM for VDAC2S, Table 1). While the 1-site model could be correct if one of the two putative receptor sites has negligible affinity for the H_0H_2 mutant, the simplest explanation is that both receptor sites likely bind to the mutant given that they bind the wild type ligand. Consistent with this, the maximum measured binding was 22000 fmol, which exceeds that predicted for a 1-site model, although with the error associated with this (8700 fmol) a single functional site cannot be excluded. Additionally, the Hill coefficients for

both models indicated no cooperativity (Table 1). These data suggest the H0+1 Pro and H2 Leu collectively promote Bax affinity for VDAC2, and contribute to conformational changes to Bax that promote positive cooperativity.

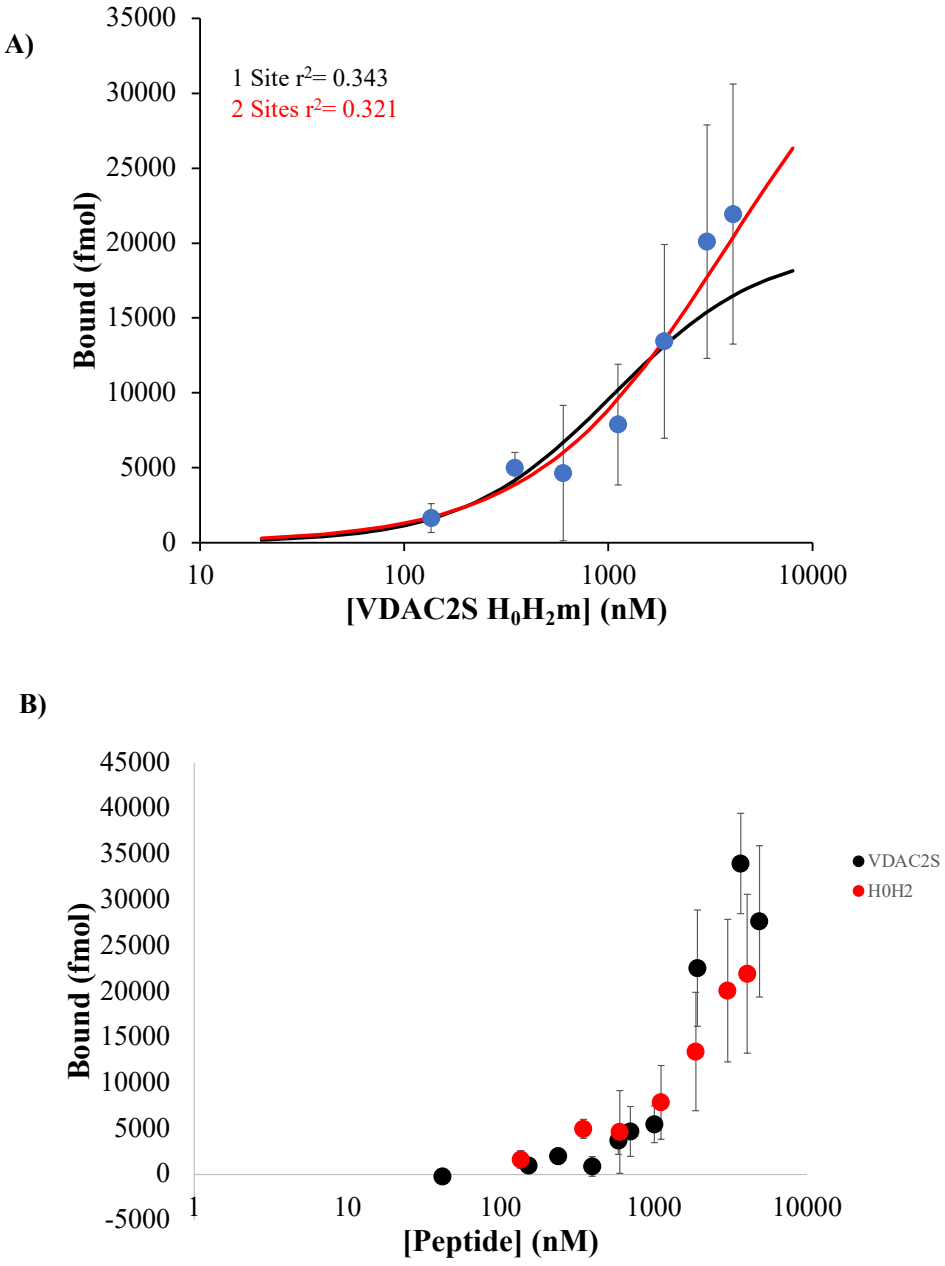

Figure 6. Bax binding to VDAC2SH_0H_2 peptides. Pro → Gly substitution at position H0+1 and Leu → Ala substitution made at H2. (A)Data are mean ± SEM of 5-8 experiments of VDAC2, with each concentration run in triplicate, represented by error bars of bound data values. Non-linear regression curves were fit to the data assuming one binding site per monomer (black, 19800 fmol B_{max}) or two sites per monomer (red, 39600 fmol B_{max}).

The correlation coefficient for each regression model is color-coded to the corresponding curve. (B) Overlay of binding curves for VDAC2S and H_0H_2 mutant peptide.

The H_1H_3 mutant consisted of Tyr → Ala and Ala → Gly substitutions (Fig 1). The purpose of these mutations was to determine the degree to which these two hydrophobic residues, Tyr and Ala at positions H1 and H3, are important in determining Bax affinity for VDAC2. The correlation coefficients for both 1- and 2-site models were similar (R^2 = 0.524; one site and R^2 = 0.573; two sites) although the maximum measured binding of 31,000 fmol (with an error of 10,000 fmol) again suggests two receptor sites in each monomer can bind this mutant. Binding affinity was modestly (1.25-fold) enhanced (2 site K_d = 1552 nM vs. 1938 nM for VDAC2S), suggesting the Tyr/Ala residues at H1 and H3 are not critical for driving Bax affinity for VDAC2S peptide. The 2-site Hill coefficient (1.4) suggested no binding cooperativity.

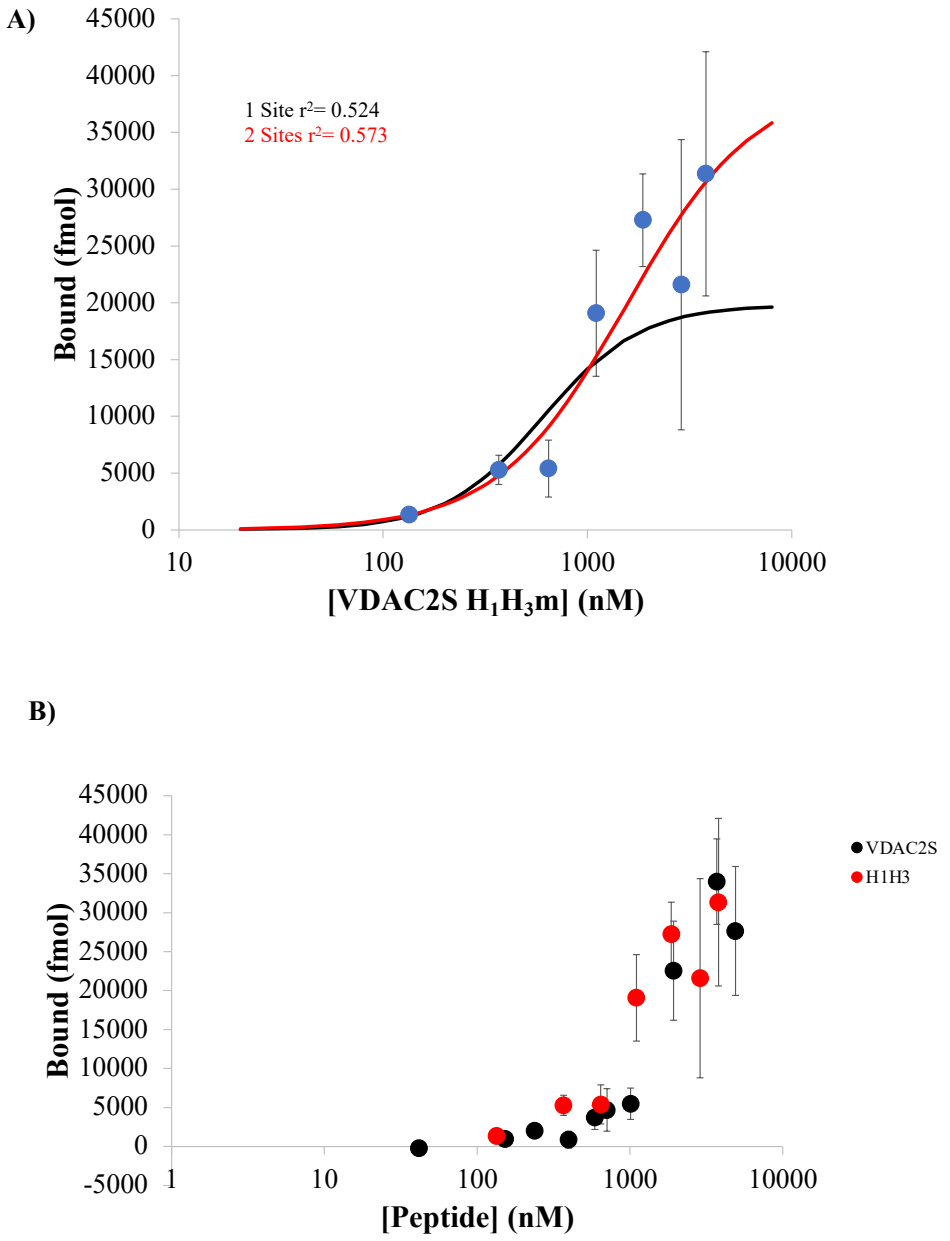

Figure 7. Bax binding to VDAC2SH$_1$H$_3$ peptides. Try → Ala substitution at position H1 and Ala → Lys substitution made at H3. (A)Data are mean ± SEM of 5-8 experiments of VDAC2, with each concentration run in triplicate, represented by error bars of bound data values. Non-linear regression curves were fit to the data assuming one binding site per monomer (black, 19800 fmol B_{max}) or two sites per monomer (red, 39600 fmol B_{max}). The correlation coefficient for each regression model is color-coded to the corresponding curve. (B) Overlay of binding curves for VDAC2S and H$_1$H$_3$ mutant peptide.

The H_2H_4 mutant containing Leu → Ala and Phe → Gly substitutions (Fig. 1) resulted in similar 1- and 2-site fits to the data (R2 = 0.499 and 0.536, respectively), but the maximum measured binding of 43000 fmol (with 6500 fmol uncertainty) is more consistent with a two receptor sites per monomer (Fig. 8). Surprisingly, the 2-site model indicated that Bax had approximately 6.8-fold higher affinity for this mutant (Table 1; K_d = 287 nM vs 1938 nM for VDAC2S), and indeed, a 1.7-fold greater affinity than the wild type Bim peptide. It is worth noting that Bim H4 is also a Phe residue, indicating that Phe at H4 in VDAC2 cannot by itself account for the lower affinity of this peptide vs. the H2H4 mutant. The Hill coefficient (1.66 for 2-site model) suggested positive binding cooperativity.

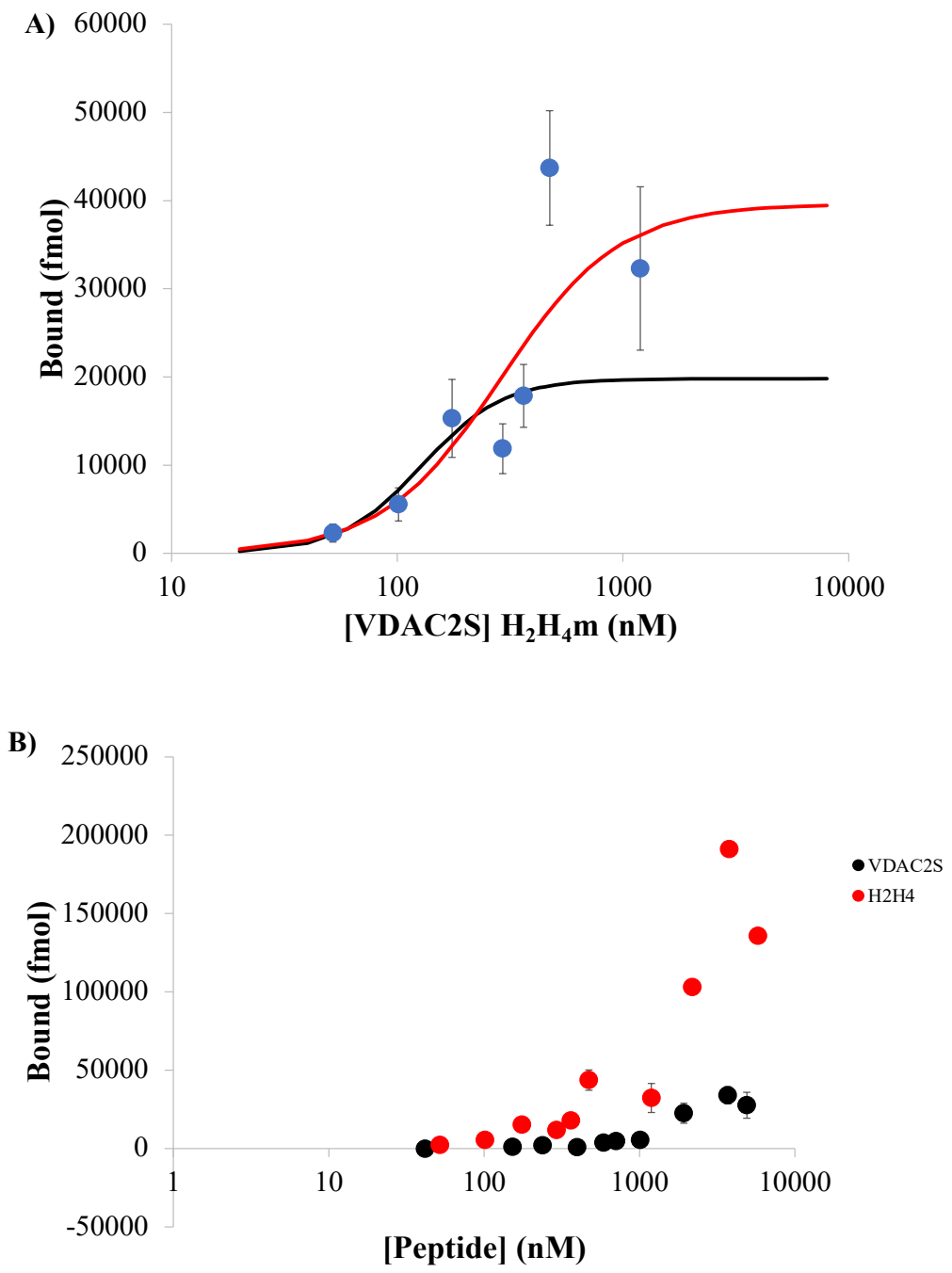

Figure 8. Bax binding to VDAC2SH$_1$H$_3$ peptides. Leu → Ala substitution at position H2 and Phe → Gly substitution made at H4. (A) Data are mean ± SEM of 5-8 experiments of VDAC2, with each concentration run in triplicate, represented by error bars of bound data values. Non-linear regression curves were fit to the data assuming one binding site per monomer (black, 19800 fmol B_{max}) or two sites per monomer (red, 39600 fmol B_{max}).

The correlation coefficient for each regression model is color-coded to the corresponding curve. (B) Overlay of binding curves for VDAC2S and H_2H_4 mutant peptide.

The H_3H_5 mutant consisted of Ala → Gly and Phe → Ala substitutions (Fig. 1). This titration yielded 1- and 2-site binding curves with virtually identical fits to the data (R2 = 0.360 and 0.369, respectively) and maximal measured binding that appeared more consistent with a single receptor site (Fig 9). Bax affinity for this mutant was either modestly higher (1.4-fold increase for 1-site model; Kd = 739 nM vs. 1048 nM for VDAC2S) or modestly lower (1.2-fold increased Kd = 2353 nM for 2-site model vs. 1938 nM for VDAC2S). This suggests the H_3H_5 residues do not substantially impact Bax binding to VDAC2S. The Hill coefficients for both the 1- and 2-site models (1.44 and 1.08, respectively) suggested no cooperativity.

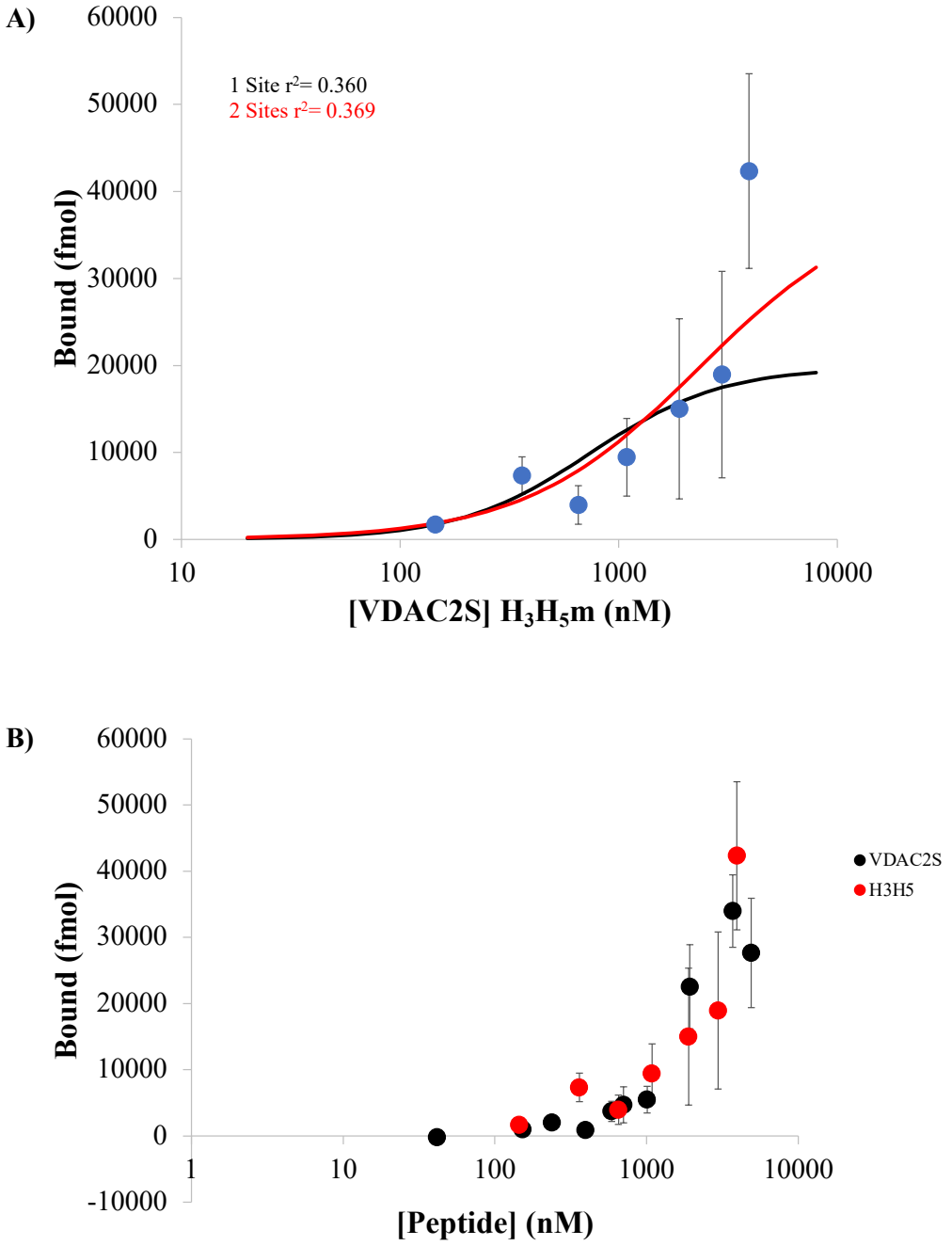

Figure 9. Bax binding to VDAC2SH$_3$H$_5$ peptides. Ala → Gly substitution at position H3 and Phe → Ala substitution made at H5. (A)Data are mean ± SEM of 5-8 experiments of VDAC2, with each concentration run in triplicate, represented by error bars of bound data values. Non-linear regression curves were fit to the data assuming one binding site per monomer (black, 19800 fmol B_{max}) or two sites per monomer (red, 39600 fmol B_{max}).

The correlation coefficient for each regression model is color-coded to the corresponding curve. (B) Overlay of binding curves for VDAC2S and H_3H_5 mutant peptide.

To test the role of the conserved Asp residue between H3 and H4, we charged swapped this residue with an Asp → Arg substitution (Fig. 1; DR mutant). The 1- and 2-site models were poor fits to the data, largely as a result of negative binding measured at 2000 nM (Fig. 10; R^2 = 0.182; and 0.184; respectively). The fits indicate this mutation reduced Bax affinity for VDAC2S by 2.5 (1-site model; Kd = 2649 nM) to 3.9-fold (2-site model; Kd = 7641 nM), indicating the conserved Asp between H3 and H4 may have a more important role in facilitating binding to Bax than any of the tested hydrophobic residues; however, the variability associated with these titrations lend more uncertainty in the measured affinities. The Hill coefficients were both close to one, suggesting no binding cooperativity (Table 1).

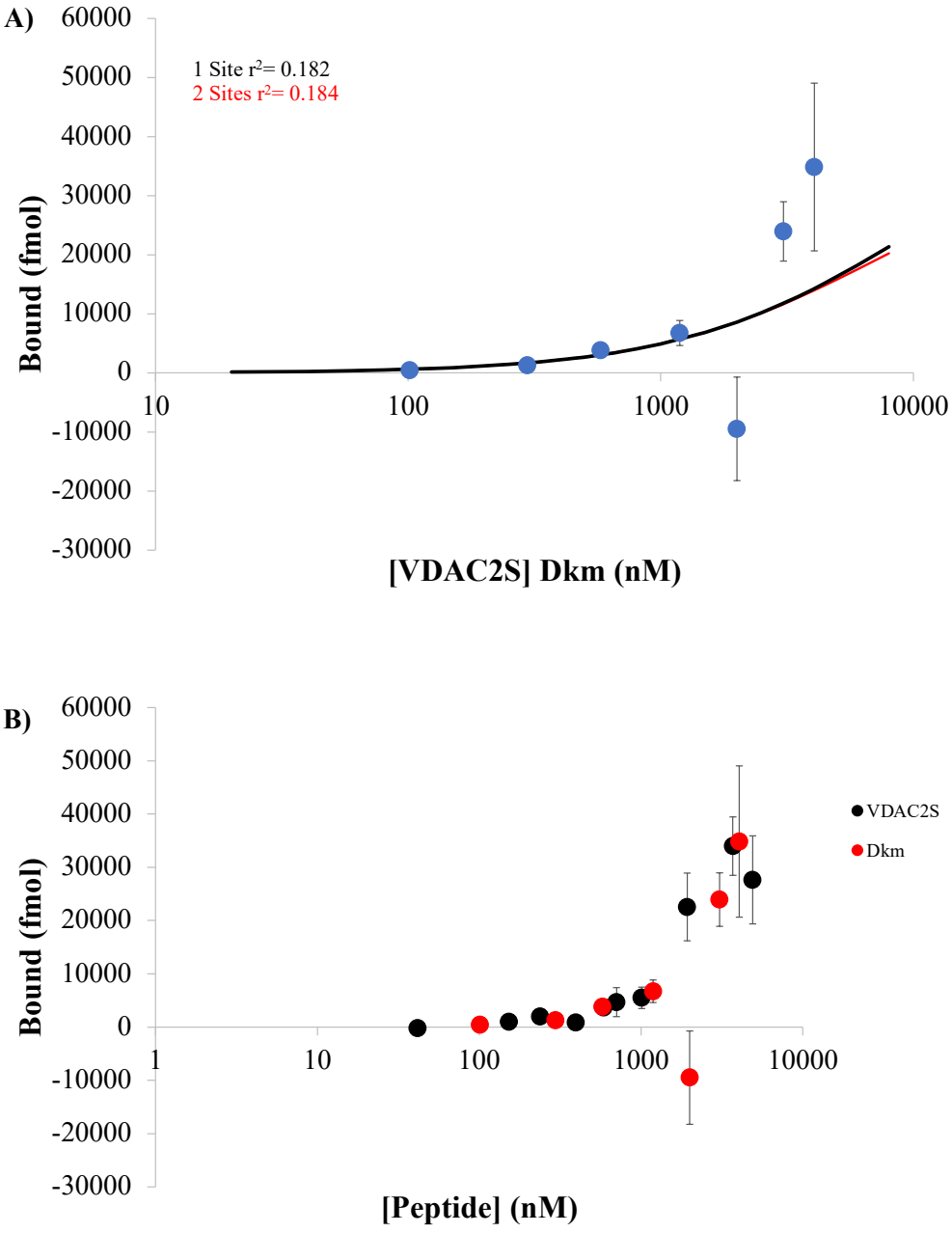

Figure 10. Bax binding to VDAC2SDR peptides. Asp → Arg substitution between H3 and H4. (A)Data are mean ± SEM of 5-8 experiments of VDAC2, with each concentration run in triplicate, represented by error bars of bound data values. Non-linear regression curves were fit to the data assuming one binding site per monomer (black, 19800 fmol B_{max}) or two sites per monomer (red, 39600 fmol B_{max}). The correlation coefficient for each regression model is color-coded to the corresponding curve. (B) Overlay of binding curves for VDAC2S and DR mutant peptide.

To test the collective role of residues H1 to H4, we generated a quadruple mutant in which each hydrophobic residue was substituted for Glu (VDAC2S 4xE mutant; Fig 1). Glutamate is a hydrophilic, negatively charged residue, which is predicted to negatively affect binding affinity as hydrophobic interactions between H1-H4 in BH3 domains and the hydrophobic groove of Bax are known to be important for high affinity binding. The 1- and 2-site models gave virtually identical fits to the data (R^2 = 0.552and 0.559, respectively; Fig 11). The highest tested peptide concentration (3600 nM) resulted in ~28000 fmol bound, suggesting two receptor sites per monomer, yet the variability between experiments was sufficiently high (standard error ~ 10500 fmol) to not allow a firm conclusion on the true number of functional sites for this peptide. Surprisingly, Bax affinity for the 4xE mutant did not substantially differ from the VDAC2S peptide, with the 2-site model yielding Kd only 1.07-fold greater (Kd = 2073 nM vs 1938 for VDAC2S; Table 1). Conversely, the 1-site model resulted in a modestly greater affinity for the 4xE mutant peptide (Kd = 761 nM vs. 1048 nM for VDAC2S). Overall, these data suggest that hydrophobic residues H1-H4 are collectively dispensable for Bax binding to the VDAC2S peptide. Hill coefficients for both the 1- and 2-site models (1.58 and 1.24, respectively) suggest no binding cooperativity.

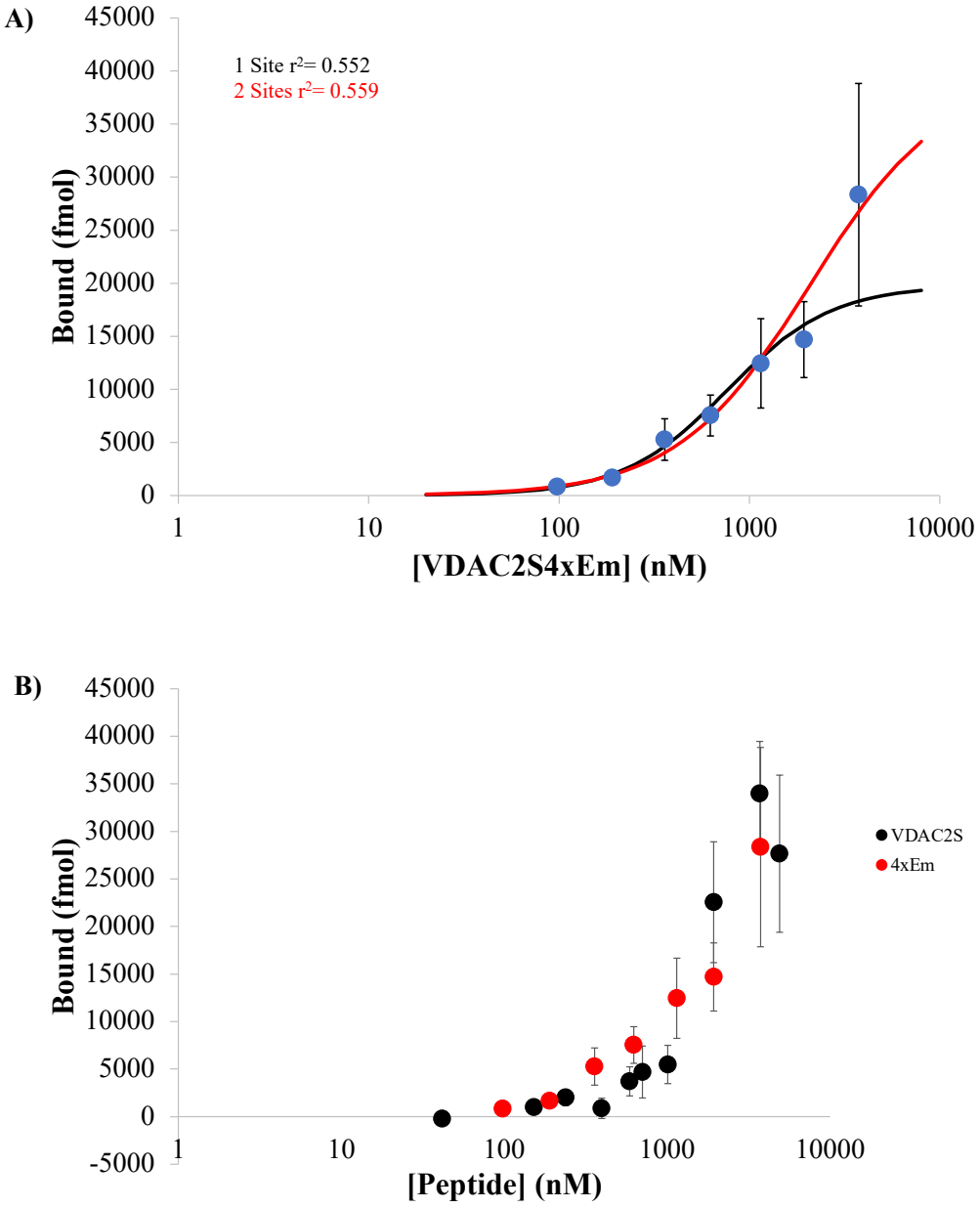

Figure 11. Bax binding to VDAC2S4xE peptide. The H1 through H4 residues were subsisted with Glu. (A) Data are mean ± SEM of 5-8 experiments of VDAC2, with each concentration run in triplicate, represented by error bars of bound data values. Non-linear regression curves were fit to the data assuming one binding site per monomer (black, 19800 fmol B_{max}) or two sites per monomer (red, 39600 fmol B_{max}). The correlation coefficient for each regression model is color-coded to the corresponding curve. (B) Overlay of binding curves for VDAC2S and DR mutant peptide.

C. Bim Blue Native Gel

Blue native gel experiments using Coomassie G250 dye were used to compare the molecular weight and possible oligomerization of WT Bim and its mutants. Results of the blue native gel electrophoresis provided information regarding the molecular weights of each peptide as well as the possible oligomerization state. Bim WT peptide had a large band at 11.5 kD, a faint band at 7.1 kD, and a third band at 3.7 kD (Fig. 12A). This suggests that the Bim WT had a molecular weight over 10 kD, which was the size of spin filter used during titrations, which is a possible reason for a smaller percentage of filtrate in the WT peptide. If the spin filters retained any peptides over 10 kDa, but allowed for filtration of peptides weighing under 10 kDa, this could have led to smaller amounts of WT filtrate and a less accurate reading. This is supported in (Fig. 12B) which shows that WT Bim only had 0.1 peptide fraction filtered. Additionally, this means that both monomeric and dimeric forms of the WT Bim were unable to pass through the filter, further skewing the results of the data collected above for this specific peptide. In future experiments, it would be worth it to preform additional experiments with a larger molecular weight spin filter, especially when dealing with WT Bim, to ensure that the WT peptide is allowed to filter during centrifugation. This would clarify results by retaining oligomers only in the filter, and yield data that is more accurate. The BimH_2 mutant showed one distinct band at 11.5 kDa, as well as a faint and thin band at 3.7 kDa (Fig. 12A). This suggests that the H_2 mutant has a similar molecular weight and oligomerization patterns to the WT Bim. Despite the similarities in molecular weight at 3.7 kDa, the H_2 mutant had a fraction filter of 0.7 (Fig. 12B) which is a much larger fraction filtered than the WT. The Bim4xE mutant had a single band present at 3.7 kDa (Fig. 12A)

and given the lack of additional bands, or the presence of a single thick band on the gel, we theorized that this mutant may have a smaller molecular weight or might need to be electrophoresed for a longer period of time to separate into distinct bands. The smaller molecular weight of this peptide suggests that it would have filtered almost completely through the 10 kDa spin filters, regardless of the amount bound, given that is was significantly smaller than the filter pore. This is supported in (Fig. 12A) which shows a fraction filter of close to 1 for the 4xE mutant. The 4xE mutant having a significantly smaller molecular weight than the other two peptides, and titration data suggested that it yielded a smaller amount bound in fmol than the WT Bim (Fig. 12A).

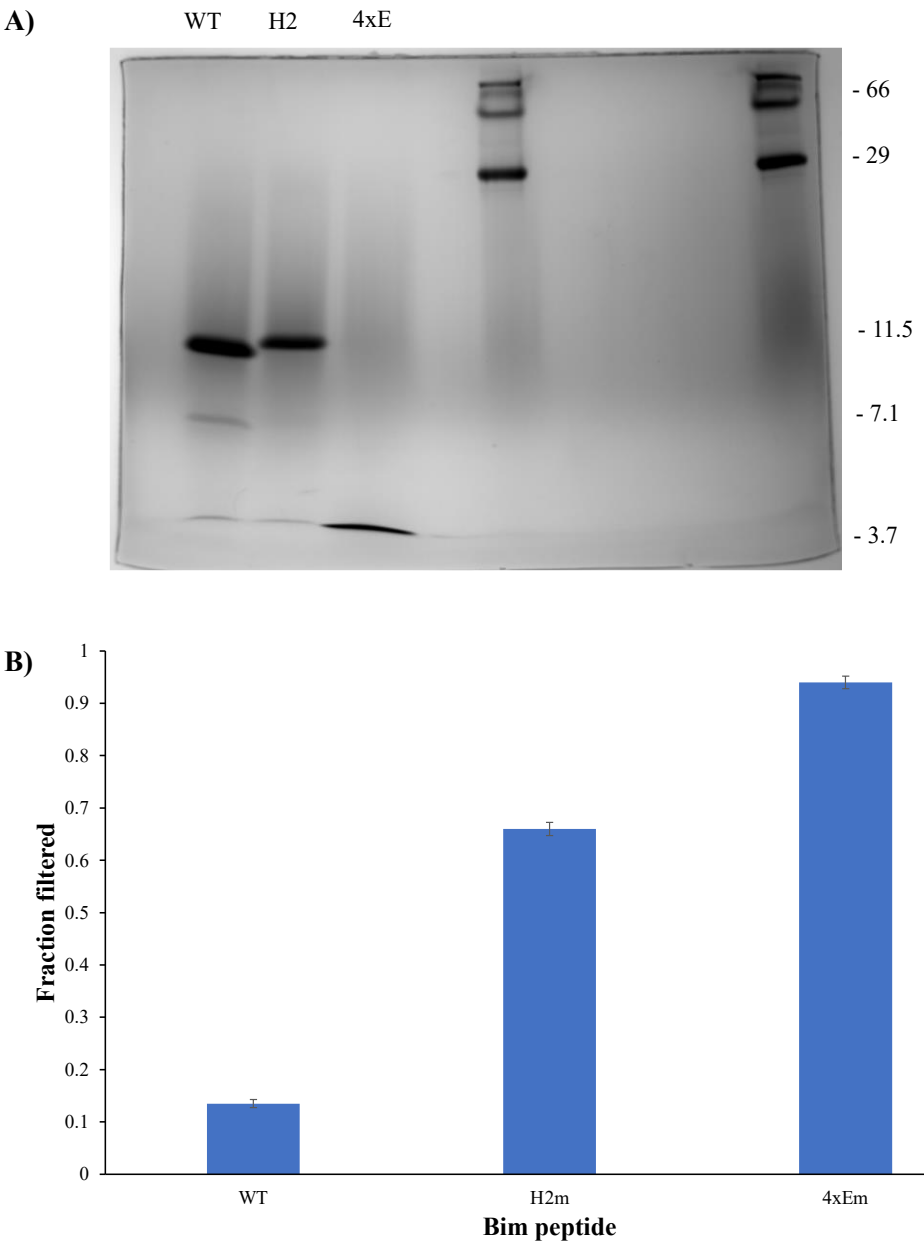

Figure 13. (A) Photographed results of Blue Native Gel Electrophoresis of Bim aggregation state. Lane 1 contains WT Bim, lane 2 contains BimH_2 mutant, lane 3 contains Bim4xE mutant, lane 4 contains 66 kD molecular marker, and lane 5 contains 66 kD molecular marker. (B) Fraction filtered of Bim WT, H_2 mutant, and 4xE mutant (figure 1A) calculated by comparing the amount of filtrate collected after being spun through 10 kDa vivaspin filters in a centrifuge to the concentration of peptide resulting from initial titration experiments. Higher fraction filtered represents less amount of peptide bound as it was able to freely move through the filter membrane. Equation: Fraction Filtered = ($[peptide]_{filtered}$) / ($[peptide]_{total}$)

Blue native gel electrophoresis (Fig. 13A). Bim WT peptide predominantly ran at ~11.5 kDa, with two faint bands at ~7.1 kDa, and ~3.7 kD, the latter of which presumably reflects monomeric peptide (Fig. 13A). This suggests that the majority of Bim WT peptide was present in a trimeric state, and thus could potentially account for the unexpectedly low fraction filtered. The BimH_2 mutant showed a similar predominant band at ~11.5 kDa, as well as a faint monomeric band at ~3.7 kDa (Fig. 12A). Despite the similarities in oligomeric state with wild type Bim, a significantly larger fraction of the H_2 mutant was filtered (Fig. 13B, 66.0 vs. 13.5 % for H2 mutant and wild type, respectively) which suggests that the fraction of peptide filtered is not simply a function of the oligomeric state on native gels. The Bim4xE mutant ran as a single 3.7 kDa band (Fig. 13A) suggesting that it largely remains monomeric in solution. Consistent with this, 94 % of the expected amount of peptide passed through the 10 kDa spin filters.

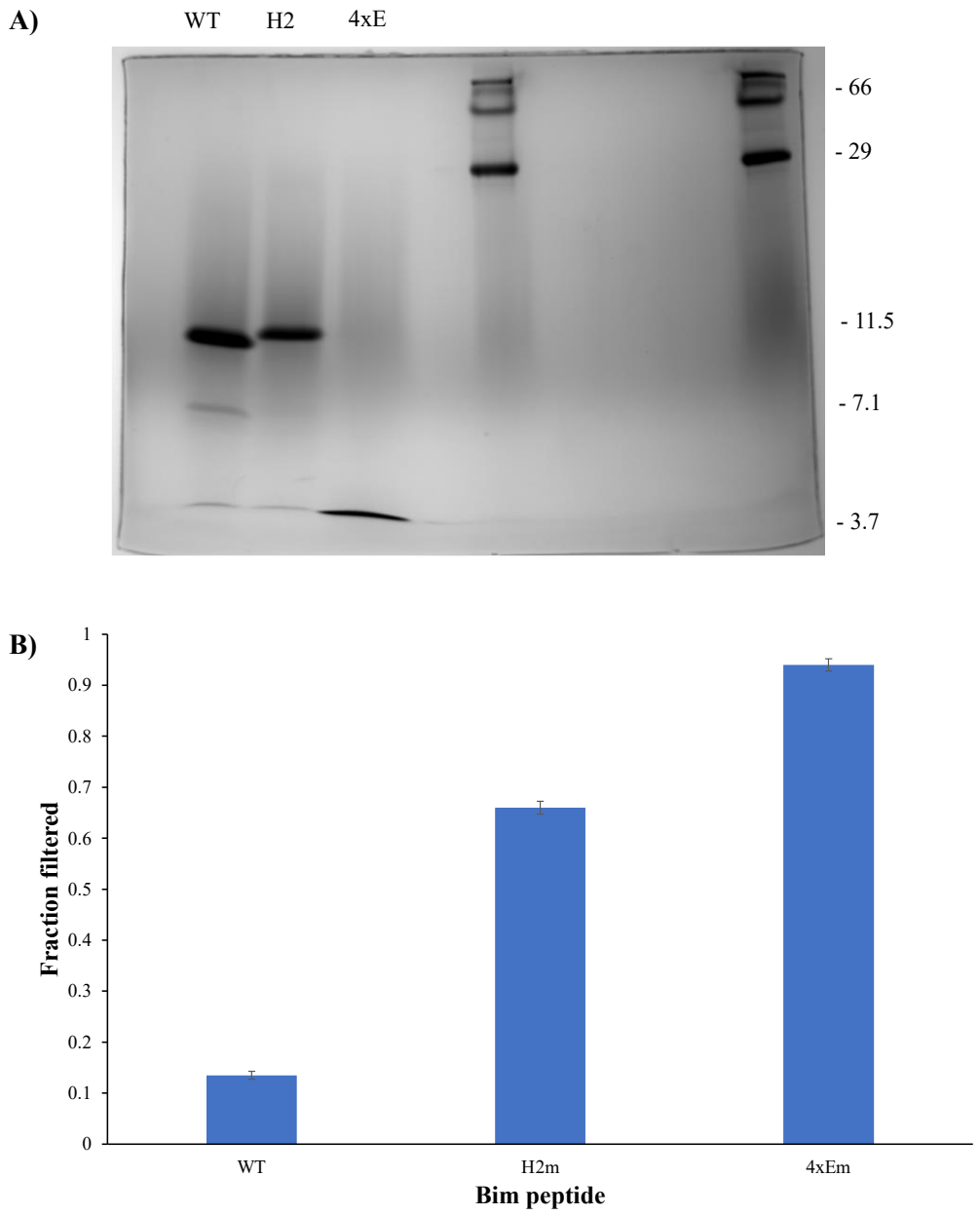

Figure 13. (A) Photographed results of Blue Native Gel Electrophoresis of Bim aggregation state. Lane 1 contains WT Bim, lane 2 contains BimH_2 mutant, lane 3 contains Bim4xE mutant, lane 4 contains (SIZE) kD molecular marker, and lane 5 contains (SIZE)kD molecular marker. (B) Fraction filtered of Bim WT, H_2 mutant, and 4xE mutant (figure 1A) calculated by comparing the amount of filtrate collected after being spun through 10 kDa vivaspin filters in a centrifuge to the concentration of peptide resulting from initial titration experiments. Higher fraction filtered represents less amount of peptide bound as it was able to freely move through the filter membrane. Equation: Fraction Filtered = ($[peptide]_{filtered}$) / ($[peptide]_{total}$)

D. VDAC2S Blue Native Gel

Similar to the Bim peptides tested, we found very low filtration fractions for most VDAC2 peptides (Fig 14B). By blue native gel electrophoresis, all VDAC2 peptides except the 4xE mutant ran between ~5-13 kDa, suggesting they annealed as dimers to tetramers in solution (Fig. 13A). The VDAC2S H_0H_2 and H_1H_3 mutants ran at ~5-9 kDa (dimer to trimer) and ~8-11 kDa (trimer), respectively (Fig. 13A) but a significantly larger fraction of the H_1H_3 mutant was filtered (Fig. 13B; 1.9 vs. 1.3 % for H_1H_3 and H_0H_2 mutants, respectively). Additionally, the H_2H_4 mutant formed what appeared to be predominantly tetramers at ~13.4 kDa (Fig. 13A) suggesting that it should have had the lowest fraction filtered, but 5.0 % of this mutant filtered, which was second highest behind the 4xE mutant (Fig. 13B), again indicating that apparent molecular weight on native gels is not the sole factor determining filtration efficiency. As with Bim 4xE mutant, the VDAC2S 4xE mutant, ran as monomer at ~3.2 kDa and had the highest filtration efficiency at 87.8 %.

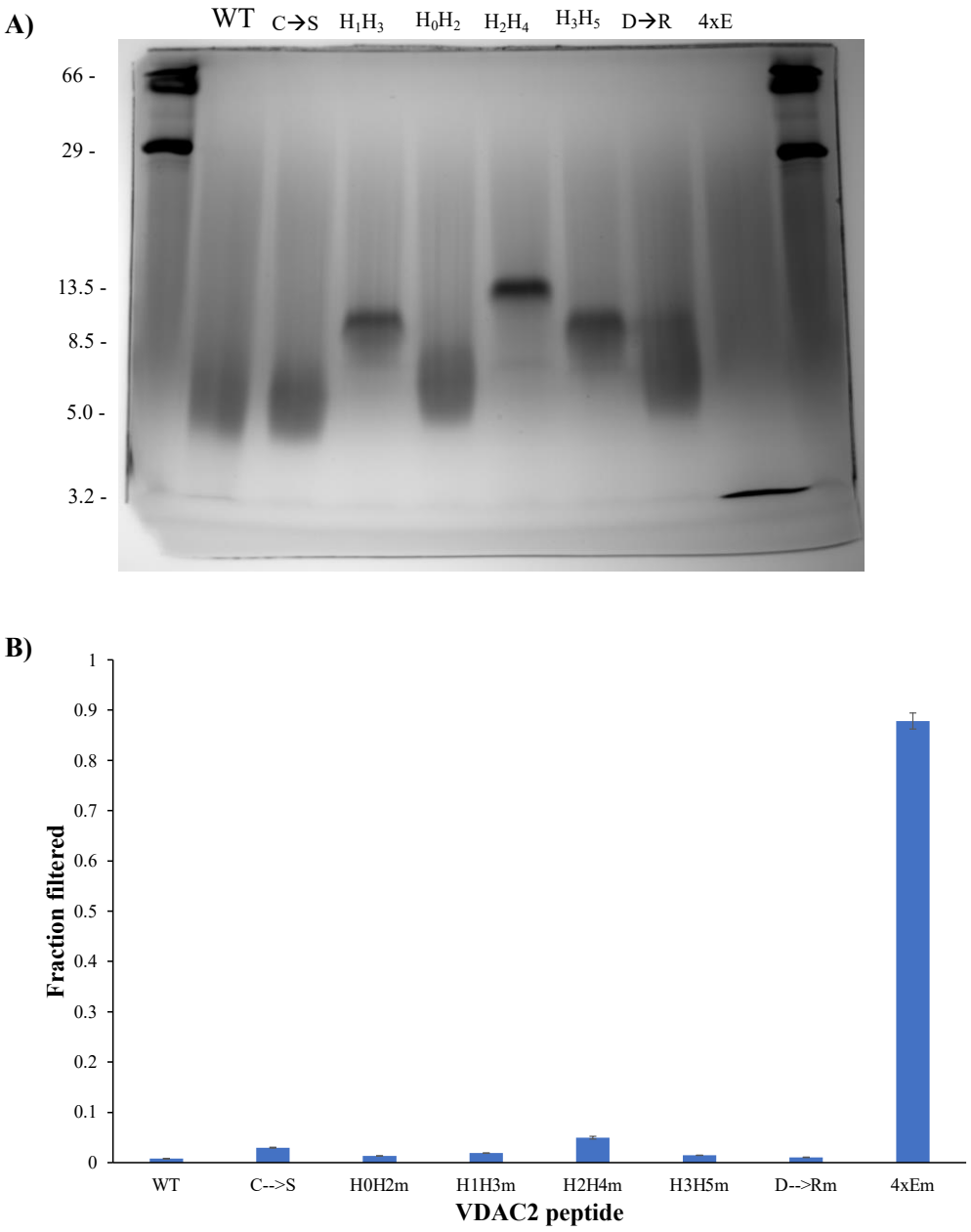

Figure 14. (A) Photographed results of Blue Native Gel Electrophoresis of VDAC2S aggregation state. Lane 1 contains a 66 kD molecular marker, lane 2 contains WT VDAC, lane 3 contains VDAC2S (WT with cys → ser mutation), lane 4 contains VDAC2SH_1H_3 mutation, lane 5 contains VDAC2SH_0H_2 mutation, lane 6 contains VDAC2SH_2H_4 mutation, lane 7 contains VDAC2SD mutation (glutamine → arginine mutation), lane 8 contains VDAC2S4xE mutation, and lane 8 contains a 66 kD molecular marker. All peptide sequences can be found in (figure 1A). (B) Fraction filtered of VDAC WT, VDAC2S, VDAC2SH_0H_2, VDAC2SH_1H_3, VDAC2SH_2H_4, VDAC2SH3H5, VDAC2SDm, and VDAC2S4xEm(figure 1A) calculated by comparing the amount of filtrate collected after being spun through 10 kDa vivaspin filters in a centrifuge to the concentration of peptide resulting from initial titration experiments. Higher fraction filtered represents less amount of peptide bound as it was able to freely move through the filter membrane. Equation: Fraction Filtered = ($[peptide]_{filtered}$) / ($[peptide]_{total}$)

DISCUSSION

The overall goal of this research aimed to determine if VDAC2 contains a functional BH3 domain that binds recombinant Bax in a manner similar to the Bim BH3 domain, a known BCL-2 protein family member. We hypothesized that VDAC2 is a novel member of the BCl-2 family due to the similarity of its N-terminal sequence to know BH3 domains. We and we tested this by comparing binding of VDAC2 peptides to a known BCl-2 family member, Bax. A BH3 domain binds to a BCl-2 family member due to the presence of conserved hydrophobic amino acid residues, as well as a conserved aspartic acid residue within the domain sequence. Potential binding of Bax to VDAC2 through a BH3 domain was tested through titration experiments and evaluated by (a) comparing the amount of peptide bound between WT and mutants, (b) comparing amount of peptide bound for both one site and two site models using non-linear regression, (c) comparing K_d, B_{max}, and hill coefficient between WT and mutant peptides. Further research was conducted to assess the possibility of different monomeric, dimeric, or trimeric conformations of the peptides through (d) blue native gel electrophoresis experiments comparing molecular weights of WT and mutant peptides. This study found that Bax binds with lower affinity to most N-terminal VDAC2 peptides than the Bim BH3 domain. The interaction exhibits some molecular features characteristic of BH3 domains, but also shows unexpected properties that indicate VDAC2 may have a non-canonical BH3 domain. The conserved aspartic acid residue between H3 and H4 is critical for Bax binding to VDAC2, as with known BH3 domains but the H1 to H4 residues in VDAC2 may not be as integral as they are in known BH3 family members.

Acknowledging the possibility of multiple binding sites per monomer of Bax is critical in interpreting the results of these experiments. Additionally, it streamlines the following analyses by focusing on either the 1- or 2-site data modeled in the non-linear regressions. Commonly, the binding site for the BH3 domain is comprised of Bax helices α2, α3, α4, and α5 forming a hydrophobic groove which, in full length Bax, is occupied by the α9 helix (Dewson et al, 2011). Little is known about the exact mechanism by which the α9 helix is displaced to expose this hydrophobic groove, so our experiments used truncated Bax lacking the final twenty amino acids that comprise the α9 helix to ensure that the hydrophobic groove is accessible to binding peptide BH3 domains. Recent research has indicated the existence of a non-canonical Bax binding site located in the region between the α1 and α6 helices (Gavathiotis et al 2008, Dengler et al., 2019). Findings of these studies indicate that at least some BH3 domains bind at the proposed α1 and α6 site to induce conformational changes that force the α9 helix out of the hydrophobic groove it rests in, thus opening the canonical Bax binding site by exposing the hydrophobic groove (Dengler et al., 2019). Another study found that binding of a BH3 activator peptide at the α1 and α6 Bax site displaces the unstructured loop between helices α1 and α2 that could be important for exposure of Bax's BH3 domain within α2 as well as release of α9 from the hydrophobic groove (Gavathoiotis et al., 2010). Physiologically, the movement of the α9 helix is essential in Bax transport from the cytoplasm to the mitochondria, and the binding of BH3 domain to the hydrophobic groove drives oligomerization and activation for cytochrome c release and triggering the apoptotic cascade (Lauterwasser et al., 2016).

Despite evidence indicating a second, non-canonical binding site on Bax, there have been no studies that have quantitatively assessed peptide binding stoichiometry to recombinant Bax. This led us to evaluate binding stoichiometries for Bim and VDAC2 peptides using both 1- and 2-site non-linear regression models. Using 110 nM Bax in 200 microliter assay volume predicts a maximal binding (B_{max}) of 19800 fmol for 1-site per monomer and 39600 fmol for 2 sites per monomer. Our findings for both peptides suggest the 2-site model better fits the data, as most titrations displayed B_{max} values greater than 20000 fmol, consistent with a second binding site on Bax that could reflect the α2-α5 hydrophobic groove and non-canonical α1/α6 sites. Thus, we consider the 2-site model K_D values to more accurately reflect Bax affinity for the peptides analyzed. The presence of two binding sites potentially complicates the interpretation of affinities since the present analysis of each peptide was sufficient to yield one K_D value. It is highly likely that the two sites have different affinities for the same peptide, so the K_D values reported most likely reflects an apparent affinity that is an average of the two sites. Moreover, any change in the apparent K_D of Bax for a mutant peptide could differ substantially from the true change in affinity of each site, especially if affinity decreases at one site but increases at the second site. While the existence of two BH3 binding sites is important to understanding Bax regulation, this discussion is focused on interpreting changes in apparent K_D of the mutants tested in the context of how the mutations could affect affinity for the hydrophobic groove receptor site since this site has been more extensively studied.

BCl-2 family proteins are integral in determining the commitment of cells to either maintaining viability or executing apoptosis. The latter process occurs when BH3-

only pro-death members of the BCl-2 family inhibit the pro-survival family members and activate Bax to induce it to oligomerize in the mitochondrial outer membrane to release cytochrome c, (Czabotar et al., 2013). BH3-only family members activate Bax, through their BH3 domains binding and triggering conformational changes to inactive Bax structure that results in self-assembly into oligomers. A conformationally activated Bax monomer undergoes multiple changes, including exposure of its BH3 domain, which drives auto-activation of other Bax monomers to facilitate oligomer formation. Alternatively, the exposed BH3 domain can interact with survival BCl-2 family members, which sequesters the BH3 α helix within the hydrophobic groove of the survival protein to prevent auto-activation and oligomer formation (Gavathiotis et al., 2010). Previous studies have discovered that Bax regulation may involve interaction with non-BCl-2 family proteins, including the mitochondrial outer membrane protein VDAC2 (Ma et al., 2014). A major goal of this study was to determine if VDAC2 contains a BH3 domain that binds Bax. This was tested through mutating residues widely accepted as being important in BH3 domain binding to the Bax hydrophobic groove. H2 and H4 residue positions are widely accepted as being important in BH3 domain binding, and these were supported by our results from the $BimH_2$ and Bim4xE mutant binding assays. The 2.9-4.3-fold lowered binding affinity in the H2 mutant, as well as the 4-5-fold lowered binding affinity for the 4xE mutant supports pervious hypothesis that these two specific residue positions are critical for BH3 domain binding in a known BCl-2 family member.

Previous studies have found that VDAC2 is essential for Bax to specifically target the MOM (Lauterwasser et al., 2016) and contains a sequence at its N-terminus that is

highly similar to a BH3 domain (Fig. 1; Pandey et al, manuscript in preparation). BCl-2 family proteins contain seven hallmark BH3 amphipathic alpha helices congregated around a central hydrophobic alpha helix (α5) (Czabotar et al., 2013). Many BCl-2 family members are known to form hydrophobic surface grooves, that can bind with multiple distinct BH3 domains (Czabotar et al., 2013). Bax, can bind the BH3 domains of multiple family members with different affinities, but only certain BH3 domains lead to conformational changes that cause activation (Czabotr et al., 2013). All BH3 domains contain hydrophobic residues at the H1 through H5 positions that are spaced such that they face the same side of the α-helix, as well as a conserved aspartic acid residue between H3 and H4. Since VDAC2 residues near the N-terminus have the same features, with the notable exception of a one residue shift in Leu at H2, our goal was to assess (a) the affinity of Bax for the N-terminus of VDAC2 using a synthetic peptide corresponding to the N-terminal sequence, and (b) the role of these residues in binding Bax by testing double mutants at positions H_0H_2, H_1H_3, H_2H_4, and H_3H_5, in addition to a single D→R mutant, and a quadruple H1/H2/H3/H4 mutant. A main finding is that Bax binds to a VDAC2 N-terminal 26 amino acid peptide, but with a 4.0-fold lower affinity compared to a Bim BH3 domain 26 amino acid synthetic peptide. The residues in VDAC2 identified as being conserved with known BH3 domains thus appear less suited for binding Bax than in the Bim BH3 domain.

One important finding from the data is that the conserved aspartic acid residue between H3 and H4 has an integral role in Bax binding to the VDAC2 peptide, as the Asp→Arg charge swap resulted in a 2.6-fold lower affinity. The conserved aspartate in the Bim BH3 domain has been shown to form a salt bridge with Arg109 within α4 of the

hydrophobic groove that is important for inducing Bax dimerization (Czabotar et al 2013). Substitution of the conserved aspartate with alanine in the Bid BH3 domain was shown to reduce Bax affinity for a Bid BH3 domain peptide by more than 5-fold (Letai et al 2002). Computational docking studies of the VDAC1 N-terminus within the hydrophobic groove is predicted to form a similar salt bridge with Arg109 (Pandey et al, manuscript in preparation). The N-terminus of VDAC2, including the aspartate between H3 and H4, is largely conserved with VDAC1, suggesting Arg109 in the hydrophobic groove is a strong candidate driving interaction with the VDAC2 peptide. The Asp → Arg mutation maintained the presence of an electrically charged side chain, however, the presence of a positively charged Arg side chain as opposed to the negatively charged Asp in the WT peptide would result in charge repulsion with Bax Arg109 and thus could be reason for lowered binding affinity.

To test the importance of the putative VDAC2 H1 to H4 residues, we determined the binding affinity of the VDAC2 4xE mutation in which the hydrophobic residues Tyr, Leu, Ala, and Phe, at H1, H2, H3, and H4, respectively, were substituted for negatively charged Glu residues. We hypothesized that this change would strongly diminish binding affinity if the four hydrophobic residues are collectively important for binding, as in many BH3 domains. Somewhat surprisingly, we found that there was only a 1.07-fold reduction in binding affinity, suggesting that collectively, these four residues may not be important in determining Bax binding affinity to the VDAC2 peptide. An alternative interpretation is that the quadruple substitution with glutamate may substantially affect the peptide secondary structure in ways that result in other hydrophobic residues driving the interaction. In addition to the H5 phenylalanine and H0 proline plus isoleucine, there

are five additional hydrophobic residues within the 4xE mutant peptide (Ala at H1+1 and H3-1, Ile at H4-1, Phe at H5+2, Leu at H5+4, and Val at H5+5). Helical wheel analysis of the 4xE mutant indicates that the H3-1 Ala, H4-1 Ile, and H5+2 Phe form a predicted hydrophobic face over 12 residues, with the conserved Asp offset from this face similar to the wild type peptide. Thus, it is possible that the 4xE mutant peptide orients differently in the hydrophobic groove such that the four glutamates at H1 to H4, which cluster together in the helix face more toward the aqueous environment while H3-1, H4-1, and H5+2 residues make hydrophobic contacts with Bax.

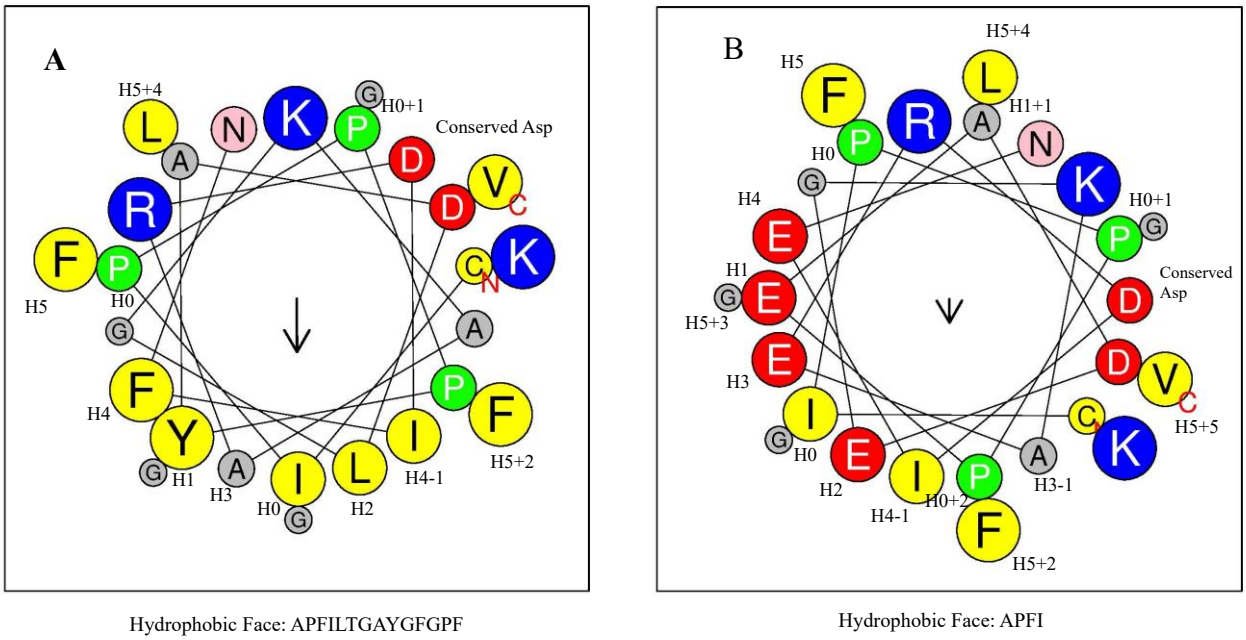

Hydrophobic Face: APFILTGAYGFGPF

Hydrophobic Face: APFI

Figure 15. (A) Helical wheel rendering of VDAC2 WT from heliquest.ipmc.cnrs.fr depicting the structure of the residues arranged in helical formation. Center arrow points towards hydrophobic groove, and residues involved in the hydrophilic phase are listed beneath the image. (B) Helical wheel rendering of VDAC24xEm from heliquest.ipmc.cnrs.fr depicting the structure of the residues arranged in helical formation. Center arrow points towards hydrophobic groove, and residues involved in the hydrophilic phase are listed beneath the image.

To further test the possibility that the putative H0 to H5 residues in VDAC2 have a role in Bax binding, we tested more conservative double mutants that may not impact

the peptide secondary structure to the extent the 4xE mutant might. For these substitutions, large hydrophobic residues were generally changed to a small hydrophobic alanine, while smaller proline or alanine were substituted with polar glycine. The H_0H_2 mutant substituted Pro→Gly at H0+1 and Leu → Ala at H2(Fig 1). Bax had a 2.0-fold lower binding affinity for this mutant (Fig. 6A) when compared to WT peptide, indicating that the proline at H0 and/or leucine at H2 may be important for the interaction between Bax and VDAC2. Computational docking studies of the VDAC1 peptide (which has the same H0+1 and H2 residues as VDAC2) to the Bax hydrophobic groove suggest that both residues may drive affinity, as the H0+1 Pro is predicted to form hydrophobic contacts with Val91 and Val95 in Bax and the H2 Leu is predicted to form hydrophobic contacts with Met79 (Pandey et al, manuscript in preparation)..

Further insight into the importance of the H0+1 and H2 residues can be obtained by comparison with the H_2H_4 mutant, in which H2 Leu→Ala and H4 Phe→Gly substitutions were used (Fig 1). Remarkably, Bax exhibited a 6.8-fold higher affinity for this mutant compared to wild type, and a 13-fold greater affinity compared to the H_0H_2 mutant, which shares the same H2 Leu→Ala substitution. In comparing the H_2H_4 to H_0H_2 mutant, the results indicate that the proline at H0+1 and/or swapping Phe for Gly at H4 is responsible for the 13-fold higher affinity of Bax for H_2H_4. Since the Pro→Gly change in H_0H_2 reduced affinity, the evidence suggests the proline at H0+1 is an important contributor to facilitating binding. Whether the H4 Phe→Gly change contributed to the stronger binding of H_2H_4 is unclear. This substitution might promote higher affinity by removal of the large aromatic Phe, thereby facilitating more effective hydrophobic interaction of Ile at H4-1, which is predicted by helical wheel analysis to reside within the

hydrophobic face of a putative VDAC2 α-helix. In comparing the 6.8-fold higher affinity of the H_2H_4 mutant to wild type, it is possible that the H2 Leu→Ala substitution also facilitates interaction with Bax. All known BH3 domains contain a strictly conserved Leu at H2, but in VDAC2 this Leu is shifted one residue closer to H1, so it is not strictly conserved. From computational docking studies, the same shift in VDAC1 is predicted to result in the H1 tyrosine (also present in VDAC2) and H2 leucine making hydrophobic contacts with the same Bax residue (Met79), whereas H1 and H2 in a known BH3 domain such as Bim make hydrophobic contacts with different Bax residues (Met79 and Met99 plus Phe116, respectively; Czabotar et al, 2013). This raises the possibility of steric interference between the large H1 Tyr and H2 Leu in VDAC2 in contacting the same Met79. From this, we propose that substituting a large leucine for small hydrophobic alanine at the shifted H2 position could relieve steric hindrance and thus promote higher affinity. The H2 Leu is thus proposed to be involved in Bax binding to VDAC2, but perhaps hinders binding compared to a smaller hydrophobic residue because of the non-conserved position within VDAC2.

For the VDAC2 H_1H_3 mutant, Tyr→Ala and Ala→Gly substitutions were made at H1 and H3, respectively. This combination resulted in a modest 1.25-fold increase in binding affinity suggesting that either these residues do not have a profound impact on binding or that the changes have antagonistic effects (one change promotes lower affinity while the other enhances affinity, with the latter effect modestly stronger than the former). Earlier we proposed that the shift of H2 Leu one residue closer to H1 Tyr may lead to steric hindrance in their interaction with Met79, so that substituting a small alanine at H2 could promote higher affinity by relieving such constraints. In a similar

way, we suggest that substituting the large aromatic H1 tyrosine with alanine will have the same affect, and thus enhance binding affinity. The effect is likely to be greater than a 1.3-fold increase in affinity given that the H_2H_4 mutant exhibited a 6.8-fold higher affinity. This implies that the H3 Ala→Gly substitution, which changes a hydrophobic residue for a polar one, is most likely an affinity lowering change. If correct, this predicts that Bax would have a significantly higher affinity for the single H1 Tyr→Ala mutant than for the current H_1H_3 double mutant.

For the H_3H_5 mutant, Ala→Gly and Phe→Ala substitutions were used at H3 and H5, respectively (Fig. 1A). These coupled mutations yielded a modest 1.20-fold lower affinity compared to the wild type peptide, consistent with the idea that the H3 alanine promotes Bax binding to VDAC2. While we cannot say with certainty if the H5 Phe→Ala substitution contributes to lowering the affinity or antagonizes the H3 substitution to enhance affinity, we speculate the latter option is more likely because (a) the decrease in affinity was small and (b) computational docking studies predict the H5 Tyr of VDAC1 contacts Val111 and Phe165 in Bax, suggesting potential steric constraints that could be relieved by replacing the large aromatic Phe in VDAC2 with small alanine. Comparison of the H_3H_5 to H_1H_3 mutant can provide further insight into the role of the H1 and H5 residues since both peptides have the same H3 Ala→Gly change. Bax has a 1.5-fold lower affinity for the H_3H_5 mutant vs. the H_1H_3 mutant. Earlier, we proposed the H1 Tyr impedes Bax binding VDAC2 by steric interference with the H2 Leu. The lower affinity of the H_3H_5 mutant is consistent with steric interference by the H1 Try. This interference is likely to cause a larger difference in affinity than seen with the H_3H_5 mutant given the large increase in affinity seen with the H_2H_4 mutant

(where steric constraint between H1/H2 is suggested to be relieved). By extension, this implies that substituting the large aromatic Phe at H5 for alanine promotes higher affinity, but this is more than offset by the Tyr at H1. The WT large aromatic Tyr at H1 and Phe at H5 (Fig. 1A) may not be as well suited as smaller hydrophobic alanines for binding to the hydrophobic groove of Bax.

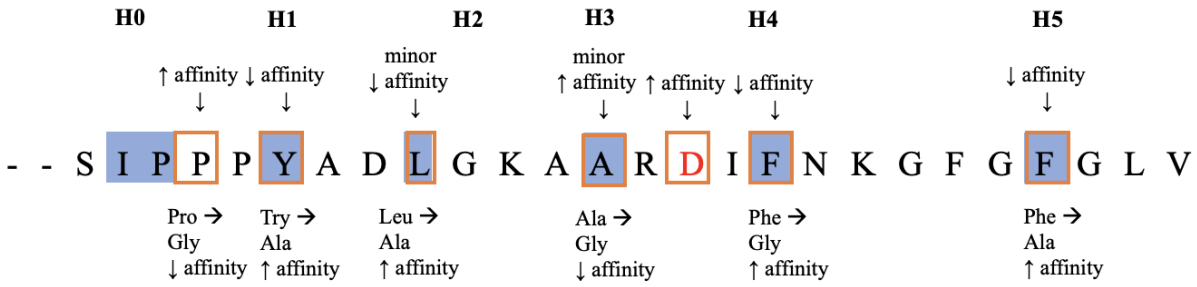

Figure 16. VDAC2 peptide sequence. Conserved residues in red font and conserved hydrophobic residues within the putative BH3 domain of VDAC are labeled H0-H5 and highlighted in blue. Summary of mutations to each residue are below the sequence, and arrow describing affinity are used to visually show effects of mutations on binding. Arrows above the sequence display hypothesized impact on binding affinity for WT residues. Note that the two affinity arrows have inverse relationships between the WT or mutant residue.

As discussed previously, a complicating factor in comparing Bax affinities for the different peptides is how the given substitutions might affect peptide structure, particularly for the quadruple 4xE mutants. One indication of potential changes in structure was the finding that the peptides differed in their ability to pass through the membranes of 10 kDa spin filters despite all of them having theoretical molecular weights between 3.2 and 3.7 kDa. A second indication of structural differences is their differing migration on blue native gels, indicative that the peptides, with the exception of the 4xE mutants, annealed to form dimers, trimers, and/or tetramers. However, the higher molecular weight species as seen on native gels did not readily correlate with lower filtration efficiency. This could be due to differences in the peptide concentrations used

for blue native gel electrophoresis (120 μM) vs that used for the titration experiments (up to 4 μM), or indicates additional factors such as peptide hydrophobicity index have a role in determining the fraction filtered. The finding that many of these peptides may predominantly exist as dimers, trimers, and/or tetramers raises the concern that Bax may be incapable of binding these oligomeric species, which raises the possibility that the true monomeric peptide concentration in these assays may be substantially lower than the nominal concentrations added. This would introduce error in the calculated amount of bound peptide, as well as into the affinity of Bax for each peptide. Further experiments in which the buffer composition for the binding experiments is varied (particularly for the type of detergent and ionic strength) are necessary to determine a condition under which these peptides predominantly remain in monomeric form.

In summary, Bax binds a VDAC2 N-terminal peptide with about a four-fold lower affinity than to the Bim BH3 domain peptide, making the N-terminus a potential domain through which VDAC2 and Bax interact. The results of this study provide insight into the relative importance of residues that constitute a putative BH3 domain within the N-terminus in binding Bax. The two most important of these that promote Bax affinity for the VDAC2 peptide are the proline at the H0+1 position and aspartate between H3 and H4. A shift in position of the H2 leucine toward H1 may create steric interference with the H1 tyrosine in their interaction with Bax Met79, as substitution of leucine with a smaller alanine appears to strongly increase Bax affinity for VDAC2. The H2 leucine shift may be a primary reason that Bax has a lower affinity for the VDAC2 peptide. The H5 phenylalanine may also not be optimal for high affinity binding, as an alanine at this position is predicted to improve binding affinity. It can be argued that VDAC2 does not

possess a BH3 domain because the shift in H2 leucine has a detrimental effect on binding Bax, and the quadruple H1-H4 4xE mutant bound nearly as well. However, the evidence that the hydrophobic residues labeled H0 to H5 and the conserved aspartate contribute to the observed binding, albeit not as tightly as with the Bim BH3 domain, suggests a rudimentary, or non-canonical, BH3 domain exists within VDAC2. Further experiments are necessary to determine if the VDAC2 peptide is an activator or inhibitor of Bax.

REFERENCES

1. Bayrhuber M, Meins T, Habeck M, Becker S, Giller K, Villinger S, Vonrhein C, Griesinger C, Zweckstetter M, Zeth K. Structure of the human voltage-dependent anion channel. Proc Natl Acad Sci U S A. 2008 Oct 7;105(40):15370-5. doi: 10.1073/pnas.0808115105. Epub 2008 Oct 1. PMID: 18832158; PMCID: PMC2557026.

2. Cheng S, Hsia CY, Leone G, Liou HC. Cyclin E and Bcl-xL cooperatively induce cell cycle progression in c-Rel-/- B cells. Oncogene. 2003 Nov 20;22(52):8472-86. doi: 10.1038/sj.onc.1206917. PMID: 14627988.

3. Czabotar, P., Lessene, G., Strasser, A. *et al.* Control of apoptosis by the BCL-2 protein family: implications for physiology and therapy. *Nat Rev Mol Cell Biol* 15, 49–63 (2014). https://doi.org/10.1038/nrm3722

4. Dengler MA, Robin AY, Gibson L, Li MX, Sandow JJ, Iyer S, Webb AI, Westphal D, Dewson G, Adams JM. BAX Activation: Mutations Near Its Proposed Non-canonical BH3 Binding Site Reveal Allosteric Changes Controlling Mitochondrial Association. Cell Rep. 2019 Apr 9;27(2):359-373.e6. doi: 10.1016/j.celrep.2019.03.040. PMID: 30970242.

5. Elmore S. Apoptosis: a review of programmed cell death. Toxicol Pathol. 2007 Jun;35(4):495-516. doi: 10.1080/01926230701320337. PMID: 17562483; PMCID: PMC2117903.

6. Gavathiotis E, Reyna DE, Davis ML, Bird GH, Walensky LD. BH3-triggered structural reorganization drives the activation of proapoptotic BAX. Mol Cell. 2010 Nov 12;40(3):481-92. doi: 10.1016/j.molcel.2010.10.019. PMID: 21070973; PMCID: PMC3050027.

7. Grant Dewson, Ruth M. Kluck; Mechanisms by which Bak and Bax permeabilise mitochondria during apoptosis. *J Cell Sci* 15 August 2009; 122 (16): 2801–2808. doi: https://doi.org/10.1242/jcs.038166

8. Hardwick JM, Soane L. Multiple functions of BCL-2 family proteins. Cold Spring Harb Perspect Biol. 2013 Feb 1;5(2):a008722. doi: 10.1101/cshperspect.a008722. PMID: 23378584; PMCID: PMC3552500.

9. Hauseman ZJ, Harvey EP, Newman CE, Wales TE, Bucci JC, Mintseris J, Schweppe DK, David L, Fan L, Cohen DT, Herce HD, Mourtada R, Ben-Nun Y, Bloch NB, Hansen SB, Wu H, Gygi SP, Engen JR, Walensky LD. Homogeneous Oligomers of Pro-apoptotic BAX Reveal Structural Determinants of Mitochondrial Membrane Permeabilization. Mol Cell. 2020 Jul 2;79(1):68-83.e7. doi: 10.1016/j.molcel.2020.05.029. Epub 2020 Jun 12. PMID: 32533918; PMCID: PMC7472837.

10. Lauterwasser J, Todt F, Zerbes RM, Nguyen TN, Craigen W, Lazarou M, van der Laan M, Edlich F. The porin VDAC2 is the mitochondrial platform for Bax retrotranslocation. Sci Rep. 2016 Sep 13;6:32994. doi: 10.1038/srep32994. PMID: 27620692; PMCID: PMC5020405.

11. Letai A, Bassik MC, Walensky LD, Sorcinelli MD, Weiler S, Korsmeyer SJ. Distinct BH3 domains either sensitize or activate mitochondrial apoptosis, serving as prototype cancer therapeutics. Cancer Cell. 2002 Sep;2(3):183-92. doi: 10.1016/s1535-6108(02)00127-7. PMID: 12242151.

12. Ma SB, Nguyen TN, Tan I, Ninnis R, Iyer S, Stroud DA, Menard M, Kluck RM, Ryan MT, Dewson G. Bax targets mitochondria by distinct mechanisms before or during apoptotic cell death: a requirement for VDAC2 or Bak for efficient Bax apoptotic function. Cell Death Differ. 2014 Dec;21(12):1925-35. doi: 10.1038/cdd.2014.119. Epub 2014 Aug 22. PMID: 25146925; PMCID: PMC4227151.

13. O'Connor L, Strasser A, O'Reilly LA, Hausmann G, Adams JM, Cory S, Huang DC. Bim: a novel member of the Bcl-2 family that promotes apoptosis. EMBO J. 1998 Jan 15;17(2):384-95. doi: 10.1093/emboj/17.2.384. PMID: 9430630; PMCID: PMC1170389.

14. Suzuki M, Youle RJ, Tjandra N. Structure of Bax: coregulation of dimer formation and intracellular localization. Cell. 2000 Nov 10;103(4):645-54. doi: 10.1016/s0092-8674(00)00167-7. PMID: 11106734.

15. Yuan Z, Dewson G, Czabotar PE, Birkinshaw RW. VDAC2 and the BCL-2 family of proteins. Biochem Soc Trans. 2021 Dec 17;49(6):2787-2795. doi: 10.1042/BST20210753. PMID: 34913469; PMCID: PMC8786305.